

Editorial Manager(tm) for Journal of Structural Engineering  
Manuscript Draft

Manuscript Number: STENG-137R1

Title: High-Force-to-Volume Seismic Dissipators Embedded in a Jointed Precast Concrete Frame

Article Type: Technical Paper

Section/Category: Concrete and Prestressed Concrete Structures

Corresponding Author: Mr Geoffrey William Rodgers, B.E (Hons)

Corresponding Author's Institution: University of Canterbury

First Author: Geoffrey William Rodgers, B.E (Hons)

Order of Authors: Geoffrey William Rodgers, B.E (Hons); Kevin M Solberg, B.S., M.E.; John B Mander, B.E. (Hons), PhD; J G Chase, B.S., M.S., PhD; Brendon A Bradley, B.E. (Hons); Rajesh P Dhakal, B.S., PhD

Abstract: An experimental and computational study of an 80 percent scale precast concrete 3D beam-column joint subassembly designed with high force-to-volume (HF2V) dampers and damage-protected rocking connections is presented. A prestress system is implemented using high-alloy high-strength unbonded thread-bars through the beams and columns. The thread-bars are post-tensioned and supplemental energy dissipation is provided by internally mounted lead-extrusion (LE) dampers. A multi-level seismic performance assessment (MSPA) is conducted considering three performance objectives related to occupant protection and collapse prevention. First, bi-directional quasi-static cyclic tests characterise the specimen's performance. Results are used in a 3D nonlinear incremental dynamic analysis (IDA), to select critical earthquakes for further bi-directional experimental tests. Thus, quasi-earthquake displacement tests are performed using the computationally predicted seismic demands corresponding to these ground motions. Resulting damage to the specimen is negligible, and the specimen satisfies all performance objectives related to serviceability, life-safety, and collapse prevention.

Suggested Reviewers:

Opposed Reviewers:

# HIGH-FORCE-TO-VOLUME SEISMIC DISSIPATORS EMBEDDED IN A JOINTED PRECAST CONCRETE FRAME

Geoffery W Rodgers<sup>1\*</sup>, Kevin. M. Solberg<sup>2</sup>, John B Mander<sup>3</sup>, J. Geoffrey Chase<sup>1</sup>, Brendon A Bradley<sup>2</sup>, Rajesh P Dhakal<sup>2</sup>.

<sup>1</sup>Department of Mechanical Engineering, University of Canterbury, Private Bag 4800, Christchurch 8020, New Zealand

<sup>2</sup>Department of Civil Engineering, University of Canterbury, Private Bag 4800, Christchurch 8020, New Zealand

<sup>3</sup>Zachry Dept of Civil Engineering, Texas A & M Univeristy, College Station, TX 77483-3136, USA

\*Corrospoding author: Ph +64-3-364 2987 ext 7092; Email: [gwr37@student.cantebury.ac.nz](mailto:gwr37@student.cantebury.ac.nz)

## ABSTRACT

An experimental and computational study of an 80 percent scale precast concrete 3D beam-column joint subassembly designed with high force-to-volume (HF2V) dampers and damage-protected rocking connections is presented. A prestress system is implemented using high-alloy high-strength unbonded thread-bars through the beams and columns. The thread-bars are post-tensioned and supplemental energy dissipation is provided by internally mounted lead-extrusion dampers. A multi-level seismic performance assessment (MSPA) is conducted considering three performance objectives related to occupant protection and collapse prevention. First, bi-directional quasi-static cyclic tests characterise the specimen's performance. Results are used in a 3D nonlinear incremental dynamic analysis (IDA), to select critical earthquakes for further bi-directional experimental tests. Thus, quasi-earthquake displacement tests are performed using the computationally predicted seismic demands corresponding to these ground motions. Resulting damage to the specimen is negligible, and the specimen satisfies all performance objectives related to serviceability, life-safety, and collapse prevention.

## KEYWORDS

High force-to-volume damper, HF2V device, lead extrusion damper, multi-level seismic performance assessment, damage avoidance design, quasi-earthquake displacement testing, incremental dynamic analysis.

## INTRODUCTION

Research and development of jointed precast concrete structures has gained considerable momentum, with significant research on the PRESSS systems (Stanton et al, 1997; Priestley et al., 1999) and Damage Avoidance Design (DAD) systems (Mander and Cheng, 1997; Holden et al, 2003; and Ajrab et al, 2004). These systems accommodate inelastic behaviour by rocking at specially detailed joints, and provide a level of seismic resistance comparable to current standards for ductile (damage-prone) structures, and remain essentially damage-free, without the excessive residual displacement, common in conventional systems. Residual displacement is critical because it can lead to complete post-earthquake loss of structural amenity. However, these systems may exhibit relatively low hysteretic energy dissipation, resulting in excessive response motion. Although this may not be an issue with long period structures, short to medium period rocking structures may undergo significantly greater displacements than conventional ductile structures (Priestley and Tao, 1993). Hence, ductile jointed precast concrete systems ideally require some supplemental energy dissipation to dissipate earthquake energy and mitigate excessive displacement response.

Energy dissipation devices of varying sophistication are available. Early applications in ductile jointed connections provided dissipation by mild steel reinforcing bars, grouted in ducts across the joint (Stanton et al, 1997). The devices proved to work well, with the grout providing a degree of buckling resistance. However, de-bonding of the bars under cyclic loading caused some stiffness degradation. Other options include tension-only mild steel

1 devices (Bradley et al, 2008) and external mild steel devices allowed to buckle (Li et al,  
2 2008).

3  
4 Each option has limitations. Mild steel devices allowed to buckle lose significant  
5 energy dissipation upon buckling, giving less dissipation on subsequent cycles. Buckling  
6 restrained devices may provide more stable resistance, but considerable residual compression  
7 forces remain upon joint closing. Residual forces can alter joint behaviour, leading to  
8 potential stiffness and/or strength loss that can result in excessive displacement demand on  
9 further seismic excitation. Mild steel devices can also suffer failure due to low-cycle fatigue  
10 and should strictly be replaced following a significant earthquake. Finally, all yielding- and  
11 buckling-based dissipators provide reduced capacity on subsequent smaller response cycles  
12 where no yielding may occur.  
13  
14  
15  
16  
17  
18  
19  
20  
21  
22  
23  
24  
25

26 Other research has looked at alternatives for providing energy dissipation to concrete  
27 structures. Pekcan et al. (1995) examined the use of elastomeric spring dampers to provide  
28 energy dissipation. Christopoulos et al (2008) developed a self-centering, energy dissipating  
29 bracing system which could be used in either concrete or steel structures, while Shen et al  
30 (1995) examine the use of viscoelastic dampers to provide seismic resistance to concrete  
31 frames. The development of passive control systems that use yielding steel braces and shape-  
32 memory alloys is detailed in Dolce et al. (2005).  
33  
34  
35  
36  
37  
38  
39  
40  
41  
42

43 High force-to-volume (HF2V) lead-based damping devices provide an attractive  
44 alternative, and consist of a central shaft with a streamlined bulge encased in lead. When the  
45 shaft moves, the lead yields due to the drag effect created by the bulge (Rodgers et al, 2007).  
46 Properly designed, these devices behave like a type of Coulomb damper with a slight velocity  
47 sensitive effect. Unlike mild steel devices, this velocity sensitivity attribute permits the HF2V  
48 device to creep back to near zero force over time, providing a reusable device with no  
49 maintenance required following an earthquake. More importantly, HF2V devices can provide  
50 the same resistive capacity every response cycle.  
51  
52  
53  
54  
55  
56  
57  
58  
59  
60  
61  
62  
63  
64  
65

1 Historically, lead-based damping devices were quite large, limiting applications to  
2 locations like base isolation (Cousins and Porritt, 1993). Recent research has developed  
3 volumetrically small devices with the same force capacity capable of direct placement in  
4 beam-column joints (Rodgers et al., 2007). As these devices have some unique manufacture  
5 and assembly attributes, they are referred to herein as a high force-to-volume (HF2V) damper.  
6  
7  
8  
9

10 Based on lead-extrusion damper (Robinson and Greenback, 1976; Cousins and Porritt,  
11 1993) and HF2V damper (Rodgers et al, 2008) tests, the velocity exponent,  $\alpha \approx 0.11-0.13$ ,  
12 where:  
13  
14  
15  
16  
17  
18

$$19 F = C_{\alpha} v^{\alpha} \quad (1)$$

20  
21  
22  
23 in which  $F$  = the damper force;  $v$  = the velocity of the shaft;  $C_{\alpha}$  = a constant dependent on the  
24 device architecture; and  $\alpha$  = the velocity exponent. More detailed velocity dependence studies  
25 can be found in Mander et al. (2009), and Rodgers (2009).  
26  
27  
28  
29  
30

31 This research incorporates the findings from previous studies (Li et al, 2008; Bradley et  
32 al, 2008; and Rodgers et al, 2007, 2008), and focuses on the development of cost effective,  
33 reliable energy dissipation and detailing schemes. Previous work related to external  
34 dissipation devices. This research places the HF2V dampers directly inside concrete beam-  
35 column joints, providing reliable energy dissipation and an architecturally pleasing finish.  
36 Detailing of the beam-ends, that frame into the column, is modified to accommodate the  
37 devices. A dual experimental-computational study investigates the seismic capacity of the  
38 proposed jointed precast concrete frame system versus the seismic demands expected from a  
39 variety of adverse earthquake scenarios.  
40  
41  
42  
43  
44  
45  
46  
47  
48  
49  
50  
51  
52  
53  
54

## 55 **SUBASSEMBLY DEVELOPMENT**

### 56 **Construction considerations**

57  
58  
59  
60 Special attention was given to potential construction issues. The beam and column  
61  
62  
63  
64  
65

1  
2  
3  
4  
5  
6  
7  
8  
9  
10  
11  
12  
13  
14  
15  
16  
17  
18  
19  
20  
21  
22  
23  
24  
25  
26  
27  
28  
29  
30  
31  
32  
33  
34  
35  
36  
37  
38  
39  
40  
41  
42  
43  
44  
45  
46  
47  
48  
49  
50  
51  
52  
53  
54  
55  
56  
57  
58  
59  
60  
61  
62  
63  
64  
65

elements were designed to be precast, with limited concrete placement required on-site. A cast in-situ ‘closure pour’ was provided at one end of each beam. The other end was considered to be a “dry-joint”. Hence: (i) tolerances could be less than fully precast members; (ii) the closure pour provides an access point for coupling the prestress thread-bars and the damping devices; and (iii) high performance concrete can be used in the high stress zone at the beam end. The closure pour thus becomes the primary focus for on-site erection. Within this region, the HF2V damper in each beam can be coupled to a threaded rod anchored in the column, the prestress thread-bars would be coupled to one another, and the channels would be tightened against the face of the column. A detailed overview of the construction sequence is given in Solberg (2007).

### **Specimen Design**

A 3D subassembly representing an interior joint on a lower floor of a ten storey building was developed. The subassembly consisted of two beams cut at their midpoints, the approximate location of the point of contraflexure for seismic loads, and an orthogonal beam designed for gravity loads. These beams were all connected to a central column. The orthogonal beam, referred to as the gravity beam, was designed to support one-way precast flooring. The other two seismic beams were designed for predominantly seismic forces. The dimensions of the prototype members were 875 mm square columns, 700 x 500 mm beams, and a 3.6m storey height. The prototype moment capacity of the beam end at the column face was 500 kNm. The subassembly was scaled to 80 percent of the prototype framed structure. The column was scaled to 700 mm square and the beams scaled to 560 mm by 400 mm. Figure 1a shows a schematic of the building from which the specimen was derived. Figure 1b shows the experimental setup, where further details on the specimen dimensions and design details may be found in Solberg (2007), Bradley et al (2008), and Li (2006). Figure 1c illustrates the reinforcing layout for the structural members, where the target longitudinal reinforcement ratio is 0.01. Note that in Figure 1c both the seismic beams are shown. These

1 beams are identical, but both are shown to provide additional section views. These members  
2 were designed to remain elastic under the expected rocking connection strength from the  
3 HF2V device and prestress forces. Four D20 ( $f_y = 500$  MPa) longitudinal threaded reinforcing  
4 bars (Reidbar<sup>TM</sup>) at the top and bottom of the beam provide a moment capacity of  $\phi M_n =$   
5  
6  
7  
8  
9 260 kNm. Due to the axial prestress load, minimal transverse steel requirements governed.  
10  
11 Thus, HR12 ( $f_y = 500$  MPa) stirrups were provided in the beam at a spacing of half the beam  
12 depth (250 mm) and a closer 100 mm spacing at the ends. Additional transverse reinforcement  
13  
14 was provided top and bottom 1.2m from the beam ends to confine the concrete in these high  
15  
16  
17  
18  
19  
20  
21  
22  
23  
24  
25  
26  
27  
28  
29  
30  
31  
32  
33  
34  
35  
36  
37  
38  
39  
40  
41  
42  
43  
44  
45  
46  
47  
48  
49  
50  
51  
52  
53  
54  
55  
56  
57  
58  
59  
60  
61  
62  
63  
64  
65

Figure 1c also illustrates the column reinforcing layout. A longitudinal reinforcement ratio of 0.01 was provided by 12 D20 ( $f_y = 500$  MPa) rebars, and transverse steel consisting of HR12 ( $f_y = 500$  MPa) stirrups at a 250 mm spacing. The stirrups were doubled and the spacing was halved within the joint region. Shear resistance was primarily provided by the core concrete, due to the axial load in the column. The stirrups were designed considering the expected overstrength of the jointed/rocking connection.

Two 45 mm longitudinal PVC ducts spaced 200 mm apart were provided for the prestress system at the seismic beam vertical centrelines. Two 26.5 mm (MacAlloy<sup>TM</sup>,  $f_y = 1100$  MPa) thread-bars provided prestress in the seismic direction utilising a straight profile to ease congestion in the column and provide a more constructible solution. The thread-bars in the gravity beam were draped to provide “load-balancing” for the gravity loading from the one-way floor panels. Hence, this thread-bar crosses the joint’s centreline at a 30 mm eccentricity.

A 300 mm cast in-situ ‘wet’ joint was provided at the column connection end of each beam. The detailing strategy in the seismic direction is shown in Figure 2a. The joint was designed to accommodate 150 x 150 mm HF2V devices at mid-height in the beam end-zone in the seismic beams, and at a 50mm vertical offset from mid-height in the gravity beam. This

1  
2  
3  
4  
5  
6  
7  
8  
offset prevents any interference between the damper anchor rods from the two orthogonal  
directions in the column. A 180mm parallel flange channel (PFC) was used top and bottom to  
armour the contact surfaces and was designed to prevent crushing of the concrete behind the  
channel from compression forces at the design moment of the joint.

9  
10  
11  
12  
13  
14  
15  
16  
17  
18  
19  
20  
21  
22  
23  
24  
25  
The channels also serve as a means of mechanically developing the longitudinal  
reinforcing, by providing cuts on the interior flange whereby the threaded longitudinal steel  
could be locked into the channel using nuts. These nuts also provided a means of ensuring the  
channel is flush with the column face during on-site fabrication. Four 25x10x500 mm rods  
were welded in the corners of each flange to help stiffen the joint region and ensure rigid  
rocking behaviour. Finally, four 1m threaded rods were spaced at 100 mm centres to provide  
attachment and anchoring points for the HF2V devices.

26  
27  
28  
29  
30  
31  
32  
33  
34  
35  
36  
37  
Shear loads were carried by four 30 mm shear keys located at each corner of the  
connecting beam. In the beam, two 30 mm holes were drilled in the top and bottom flange to  
provide a female attachment for the shear keys. The shear keys were tapered inward 5 degrees  
to prevent binding with the beam during connection opening. In the column, these shear keys  
were designed to be screwed into a nut located behind a hole in the column's steel plates.

38  
39  
40  
41  
42  
43  
44  
45  
46  
47  
48  
49  
50  
51  
52  
53  
54  
55  
56  
57  
58  
59  
60  
61  
62  
63  
64  
65  
One of the primary objectives of this study was to improve beam-column joint detailing  
by improving constructability and reducing materials compared to past designs (Li et al,  
2008). Figure 2b show that column detailing was improved by: (i) the column contact plates  
were reduced from a single full depth plate to two end plates; (ii) the prestress ducts ran  
straight, rather than angled, reducing congestion; and (iii) the internal dampers were  
connected using a single rod with grouting tubes. The column end plates were sized to  
provide a full contact surface for the beam armouring, and provide a 10 mm extension on all  
sides. This plate was checked to ensure concrete crushing in the column did not occur at the  
design strength of the connection, and was developed into the joint core using weld studs.



## Specimen construction

1           The specimen was constructed in several parts. First, the two seismic beams were caged  
2  
3  
4 with a cast insitu end, as shown in Figure 3a. This task required providing stubs for the  
5  
6 longitudinal steel, the prestress system ducts, and the threaded rods for the HF2V damper.  
7  
8 Next, the gravity beam and column were caged and cast. The gravity beam required the  
9  
10 draped profile to be located, and the damper and tendons were offset 30 and 50 mm from  
11  
12 centreline respectively to avoid intersecting the orthogonal ducts in the column.  
13  
14

15  
16           The column longitudinal reinforcement was welded to a 20 mm steel plate at the top  
17  
18 and bottom, and the armouring plates were developed into the concrete by welds studs. A  
19  
20 50mm recess at the column face where the damper anchoring rods are bolted allowed easy  
21  
22 bolt clearance. Corrugated steel tubing provided the damper ducts where the shaft and  
23  
24 connecting rods passed through. Grout tubes are provided to grout the anchoring rod within  
25  
26 the column, and the damper duct in the beam ends was left open to allow free movement of  
27  
28 the damper shaft.  
29  
30

31  
32           The remaining elements were installed to enable the closure pour, as seen in Figure 3b.  
33  
34 Within the closure pour, the HF2V devices were attached to the threaded rods in the beam.  
35  
36 The damper shaft was coupled to the threaded rod in the column, which was anchored against  
37  
38 a steel washer in the recess on the column face. The damper shaft, coupler, and column  
39  
40 threaded rod were all encased in a duct and waterproofed from the concrete.  
41  
42  
43

44  
45           Once the damper was in place the main prestress thread-bars were coupled together.  
46  
47 Next, the channel top and bottom was tightened against the column face and locked with  
48  
49 longitudinal steel nuts. Finally, a thin sheet provided a barrier between the wet concrete and  
50  
51 the column face to prevent any bonding. Note that this measure may not be necessary, since  
52  
53 the tensile capacity of the concrete would be negligible, and was taken merely as a precaution.  
54  
55

56  
57           A high performance concrete mix designed for good workability and high strength was  
58  
59 used for the three closure pours. Steel fibres (2 percent by weight) were incorporated to help  
60  
61  
62

1  
2  
3  
4  
5  
6  
7  
8  
9  
10  
11  
12  
13  
14  
15  
16  
17  
18  
19  
20  
21  
22  
23  
24  
25  
26  
27  
28  
29  
30  
31  
32  
33  
34  
35  
36  
37  
38  
39  
40  
41  
42  
43  
44  
45  
46  
47  
48  
49  
50  
51  
52  
53  
54  
55  
56  
57  
58  
59  
60  
61  
62  
63  
64  
65

impede crack propagation. This concrete had a measured 28-day compressive strength of 76 MPa, with 50 MPa measured for the regular beam and column concrete.

### The HF2V dampers

The HF2V damper designs are shown in Figure 4a. Damper shaft motion plastically extrudes lead between the shaft and outer body to dissipate energy as seen in Figure 4b (Rodgers et al, 2007). A single HF2V damper is placed within each beam end, as seen in Figure 2a. The damper shaft (Figure 4a) was designed to be coupled to a threaded rod in the column of the same size. Four 18mm ( $f_y = 300\text{MPa}$ ) threaded rods at 100mm centres were cast into the precast beam to anchor the device within the closure pour, via oversize attachment holes on the devices that allow adjustment when coupled to the threaded rod.

To ensure the system re-centres, the expected negative moment contribution from the HF2V device in compression should not exceed the expected positive moment contribution from the prestress. Hence, the moment contribution ratio,  $\lambda$ , must be greater than 1.

$$\lambda = \frac{\phi M_{PS,i}}{\Omega_{diss} M_{diss}} > 1 \quad (2)$$

where  $M_{PS,i}$  = moment contribution from the initial prestress force;  $M_{diss}$  = moment contribution from the dissipation devices in compression;  $\Omega_{diss}$  = overstrength factor of the dissipation devices (taken as 1.5);  $\phi$  = understrength factor for the prestress (taken as 0.85). Rearranging terms gives a ratio of moment contribution from prestress and HF2V devices. Initial post-tensioning of 250kN per thread-bar gives a total of 500 kN at the interface. The dampers were designed for a 250kN yield force, corresponding to  $\lambda = 1.23$  and 1.06 in the North-South direction for positive and negative moment, respectively, and  $\lambda = 1.13$  in the East-West direction.

Figure 4b presents experimental force-displacement responses of the HF2V devices in a universal (Avery<sup>TM</sup>) testing machine. Devices 1, 2 and 3 were installed in the west, east and

1 south joints of the specimen, respectively. The devices provide similar response, with an  
 2 average yield force of 270kN. Differences in initial stiffness and yield force can be attributed  
 3 to small voids forming in the lead due to incomplete pre-stressing to remove micro-voids,  
 4 where Rodgers et al (2007) discusses this issue in detail.  
 5  
 6  
 7  
 8  
 9

## 10 **PREDICTED RESPONSE**

11 The analytical prediction method assumes members remain elastic and that once gap-  
 12 opening of the beam-to-column joints occurs, displacements can be determined from rigid-  
 13 body kinematics. Taking the internal moment arm ( $e_{PS}, e_{diss}$ ) from the rocking edge and  
 14 summing each contribution:  
 15  
 16  
 17  
 18  
 19  
 20  
 21  
 22

$$23 \quad M = \sum M_{PS} + \sum M_{diss} \quad (3)$$

24 where  $M_{PS}$  = moment in the thread-bars ( $=P_{PS}e_{PS}$ ), and  $M_{diss}$  = moment in the dissipation  
 25 device ( $=P_{diss}e_{diss}$ ). The force in the thread-bars is then obtained from:  
 26  
 27  
 28  
 29  
 30  
 31  
 32  
 33

$$34 \quad P_{PS} = P_i + \frac{A_{PS}E_{PS}}{L_t} e_{PS} \theta_{con} n \quad (4)$$

35 where  $P_i$  = initial post-tensioning force (250 kN);  $E_{PS}$  = thread-bar elastic modulus  
 36 (170 GPa);  $A_{PS}$  = thread-bar cross sectional area (552 mm<sup>2</sup>);  $L_t$  = unbonded length of thread-  
 37 bar (9 m);  $\theta_{con}$  = connection rotation; and  $n$  = number of joint openings spanned by the thread-  
 38 bar (2 in the East-West direction and 1 in the North-South direction). The force in the HF2V  
 39 device is thus:  
 40  
 41  
 42  
 43  
 44  
 45  
 46  
 47  
 48  
 49  
 50  
 51  
 52  
 53

$$54 \quad P_{diss} = \min \left| \begin{array}{l} K_{diss} e_{diss} \theta_{con} \\ P_{y,diss} \end{array} \right. \quad (5)$$

55 where  $K_{diss}$  = stiffness of the dissipation device taken as 200kN/mm, which was the average of  
 56  
 57  
 58  
 59  
 60  
 61  
 62  
 63  
 64  
 65

the three devices; and  $P_{y,diss}$  = “yield force” of the HF2V device (250kN).

Given an elastic moment-curvature analysis, the force-displacement response of the subassembly can be evaluated. In the East-West direction, the horizontal force at the top of the column,  $V_{col}$ , can be found given the moment at the joint:

$$V_{col} = 2M \frac{L}{L_b L_c} \quad (6)$$

where  $L$  = beam length to column centreline (9.8m);  $L_b$  = clear support length of the beam (9.1m); and  $L_c$  = storey height (2.8m). The total top displacement of the system, given  $V_{col}$ , can be attributed to localised joint rotation and the total elastic deformation of the system:

$$\Delta = \Delta_{elastic} + \theta_{con} \frac{L_b}{L} L_c \quad (7)$$

in which  $\Delta_{elastic}$  = the elastic deformation of the system from flexure, given by:

$$\Delta_{elastic} = \frac{V_{col,uplift}}{12} \left[ \frac{(L_c - D)^3}{EI_{col}^*} + \frac{L_c^2 L_b^3}{L^2 EI_{bm}^*} \right] \quad (8)$$

where  $EI_{bm}^*$  and  $EI_{col}^*$  are the effective stiffness of the beam ( $0.25EI_{bm, gross}$ ) and column ( $0.6EI_{col, gross}$ ), respectively; and  $D$  = the depth of the beams (560mm). A more detailed derivation of Equation (8) can be found in either Li (2006) or Rodgers (2009).

## EXPERIMENTAL SETUP

The experimental test setup shown in Figure 1b is closely similar to that in Bradley et al (2008). The column was pinned to the floor using a universal joint. Additional pins were on stiff struts near the end of each beam. Actuators A and B were located at the top of the east and south face of the column, inducing displacements in the seismic and gravity directions, respectively. Actuator C was orthogonal to the side face of the gravity beam, in line with the

1 gravity beam support strut, and was used primarily to stabilize the specimen. Rotary  
2 potentiometers were installed against the opposite face of each actuator. An additional  
3 actuator at mid height of the gravity beam simulates the precast one-way floor panels, with a  
4 constant 120kN load spread over a 1.5m timber block.  
5  
6

7  
8  
9 At one end of each prestress thread-bar anchor, load cells measure the forces in the  
10 thread-bars. Four 32 mm high strength thread-bars along the longitudinal column axis were  
11 stressed to 500 kN for a 2000 kN total axial load ( $0.1f'_cA_g$ ), simulating gravity forces. A total  
12 of 24 potentiometers measured localized displacements. Within the joint, each coupler  
13 connecting the HF2V shaft to the threaded rod in the column was converted to a load cell,  
14 consisting of eight strain gauges compensating for bending and temperature effects. Four  
15 strain gauges were placed on the top and bottom web of the beam armouring channels to  
16 detect any potential yielding upon gap-opening.  
17  
18  
19  
20  
21  
22  
23  
24  
25  
26  
27  
28  
29

## 30 TEST METHODS

31  
32  
33 Displacement controlled uni- and bi-directional testing was performed. Both quasi-static  
34 testing using cyclic loading patterns and quasi-earthquake displacement (QED) tests (Dutta et  
35 al., 1999) using load patterns from computational simulation of the full 10-storey prototype  
36 structure were employed. The QED method is intended to produce realistic displacement  
37 demands representative of expected seismic response (Dhakal et al, 2006)  
38  
39  
40  
41  
42  
43  
44  
45

### 46 Quasi-static displacement profiles

47  
48 Preliminary, low drift level quasi-static tests were used to characterise the specimen for  
49 use in a computational model for the QED test (Solberg, 2007). Owing to the damage-free  
50 nature of the specimen, it was possible to conduct preliminary tests (both uni- and bi-  
51 directional) without damaging the specimen. Further quasi-static testing was carried out  
52 following the QED testing regime, consisting of uni-directional tests in each direction to a  
53 maximum drift of 3 percent (equivalent to a radial drift of 4 percent), and bi-directional tests  
54  
55  
56  
57  
58  
59  
60  
61  
62  
63  
64  
65

to a maximum (radial) drift of 4 percent.

### **Quasi-earthquake displacement testing**

The QED method is intended as a more realistic protocol, capturing specimen behaviour under ‘real’ earthquake ground motion. Unlike quasi-static testing, which uses controlled cyclic displacements in ascending order, QED testing captures small loading cycles following severe displacement demand from initial pulses. Second, P- $\Delta$  effects can be considered in the analytical model, thus capturing non-uniform displacements due to excessive yielding in a single direction. Finally, QED test performance can be extrapolated to infer likely damage at multiple levels of excitation.

Quasi-static test data was used to create an equivalent computational model of the specimen. Details of the development of the 3D analytical model are given in Bradley et al. (2008). Elasto-plastic and bi-linear elastic springs represent the dampers and prestress at the joint, respectively. The natural period of the full structure was found to be 1.5s.

In order to perform a Multi-Level Seismic Performance Assessment (MSPA), the earthquake records to be used must be pre-identified. Dhakal et al. (2006) proposed a methodology based on Incremental Dynamic Analysis (IDA), where an IDA is conducted using multiple earthquake ground motions and the IDA results are probabilistically processed to select records that give medium and high confidence at desired levels of seismic intensity. Performing an IDA involves conducting nonlinear dynamic analyses of a computational structural model subjected to a suite of earthquake ground motion records scaled to different intensity measures (IMs) (Vamvatsikos and Cornell, 2002). For each analysis, an engineering demand parameter (EDP) is monitored, producing an IDA curve (i.e. a plot of IM vs EDP) for each earthquake record.

A reliable computational model of the structure yields displacement profiles at nodes of interest for use in physical testing. This task required the identification of earthquakes likely to represent various levels of demand, considering both rare and relatively frequent

1 earthquakes. The procedure described by Dhakal et al. (2006) was adopted to define three key  
2 earthquake records representing multiple levels of seismic demand, by performing an IDA  
3 (Vamvatsikos and Cornell, 2002) to identify the structural response from various earthquakes.  
4 Earthquakes representing percentile levels at various intensities can then be identified and  
5 used for subsequent analysis.  
6  
7  
8  
9

10 Assuming a firm soil site in Wellington, New Zealand (a high seismic zone) three levels  
11 of demand were identified following Dhakal et al. (2006). These demand levels were: (i) a  
12 90<sup>th</sup> percentile design basis earthquake (DBE); (ii) a 50<sup>th</sup> percentile maximum considered  
13 earthquake (MCE); and (iii) a 90<sup>th</sup> percentile MCE. The DBE and MCE were defined as  
14 earthquakes with return periods of 475 years (10% in 50 years) and 2475 years (2% in 50  
15 years), respectively. For the site of interest, this corresponds to a peak ground acceleration  
16 (PGA) of approximately 0.4g for the DBE and 0.8g for the MCE, based on the seismic hazard  
17 model in Stirling et al. (2002). For each demand level, a performance level related to  
18 serviceability and life-safety was defined. For the 90<sup>th</sup> percentile DBE it corresponds to a high  
19 level of confidence that the structure remains operational. After the MCE the structure is  
20 expected to be repairable with a moderate level of confidence (50<sup>th</sup> percentile MCE) and is  
21 not expected to collapse with a high level of confidence (90<sup>th</sup> percentile MCE).  
22  
23  
24  
25  
26  
27  
28  
29  
30  
31  
32  
33  
34  
35  
36  
37  
38  
39

40 Earthquake records were selected from a suite of 20 recorded ground motions from the  
41 SAC project (Sommerville et al., 1997). The spectral acceleration ( $S_a$ ) at the fundamental  
42 period of the structure was selected as the intensity measure (IM) (Baker and Cornell, 2005).  
43 Thus, the DBE and MCE intensity levels correspond to a  $S_a$  of 0.27g and 0.48g, respectively.  
44 The resulting IDA data is plotted in Figure 5, showing the 10<sup>th</sup>, 50<sup>th</sup>, and 90<sup>th</sup> percentile  
45 curves, which notes the three selected records. These records correspond to peak (radial)  
46 interstory drifts of 1.6, 1.6 and 2.8 percent for the 90% DBE, 50% MCE, and the 90% MCE,  
47 respectively.  
48  
49  
50  
51  
52  
53  
54  
55  
56  
57  
58  
59  
60  
61  
62  
63  
64  
65

## EXPERIMENTAL RESULTS

1  
2 This section first presents results from the quasi-static tests, followed by QED test  
3  
4 results.  
5  
6

### 7 8 **Quasi-static test results** 9

10 The response of the subassembly in the East-West and North-South direction is given in  
11 Figure 6. The specimen was subjected to two fully-reversed displacement cycles, at column  
12 drift amplitudes of 0.5, 0.75, 1.5, 2.25, and 3.0 percent. The prediction using Equations (3) to  
13 (8), is plotted along with the experimental results, with good agreement between the two.  
14  
15  
16  
17  
18  
19

20 In the East-West direction, the hysteretic behaviour displays notable energy dissipation.  
21 The dissipation is notably high, given that the structural members remain essentially elastic,  
22 and therefore provides essentially no hysteretic energy dissipation. Furthermore, the straight  
23 tendon profile in the East-West (seismic) direction results in very low friction between the  
24 duct and tendons and therefore also contribute very little inherent energy dissipation. The  
25 hysteretic results without damper contributions are presented in Rodgers (2009), and show an  
26 essentially bi-linear elastic response regime with negligible energy dissipation. The specimen  
27 did not suffer any noticeable stiffness or strength degradation, and stable hysteretic energy  
28 dissipation is evident. The maximum recorded residual drift was approximately 0.08%, (2.6%  
29 of the maximum drift), and is attributed to friction arising within the prestressing system.  
30  
31  
32  
33  
34  
35  
36  
37  
38  
39  
40  
41  
42  
43

44 In the North-South direction, the results are similar, with stable energy dissipation. The  
45 maximum residual drift was 0.12%, (4% of the maximum). This value is slightly larger than  
46 the East-West direction, and is attributed to the increase in prestress friction from the draped  
47 tendon profile. Differential friction forces due to reversed cyclic loading contribute to this  
48 effect.  
49  
50  
51  
52  
53  
54  
55

56 These frictional effects can be clearly seen in Figure 7a, which shows the change in  
57 prestress force for a given column displacement. It is evident that friction between the duct  
58  
59  
60  
61  
62  
63  
64  
65



1 and prestress thread-bars leads to some energy dissipation not considered in the original  
2 design. This effect is minimised in the East-West direction, where the straight ducts result in  
3 less tendon-duct friction. Figure 7b shows the ‘in-service’ response of the HF2V damper in  
4 the east beam. The apparent in-service stiffness of the damper was reduced compared to the  
5 damper tests alone. It is very important to note that the displacement in Figure 7b is not  
6 directly measured, but rather an inferred displacement measured across the joint at the beam  
7 mid height by a potentiometer attached to the column face. It therefore records the mid-height  
8 gap-opening displacement and includes all sources of flexibility from axial stretching of the  
9 connecting elements to take-up in the threaded coupler nuts. Due to the embedded device  
10 design, direct in-service device displacements were unavailable. These additional sources of  
11 flexibility and slackness reduced the contribution of the damper to the overall hysteretic  
12 performance on smaller cycles. For example, the HF2V device should “yield” at  
13 approximately 1 mm of elongation, but was not observed until ~2.5 mm. The revised stiffness  
14 of the HF2V devices considering the added freedom in the connecting elements is  
15 ~80 kN/mm and 50 kN/mm for the gravity and East-West joints, respectively. Improved  
16 detailing of device connections will reduce or eliminate this behaviour.

17  
18  
19  
20  
21  
22  
23  
24  
25  
26  
27  
28  
29  
30  
31  
32  
33  
34  
35  
36  
37  
38  
39  
40  
41  
42  
43  
44  
45  
46  
47  
48  
49  
50  
51  
52  
53  
54  
55  
56  
57  
58  
59  
60  
61  
62  
63  
64  
65  
66  
67  
68  
69  
70  
71  
72  
73  
74  
75  
76  
77  
78  
79  
80  
81  
82  
83  
84  
85  
86  
87  
88  
89  
90  
91  
92  
93  
94  
95  
96  
97  
98  
99  
100  
101  
102  
103  
104  
105  
106  
107  
108  
109  
110  
111  
112  
113  
114  
115  
116  
117  
118  
119  
120  
121  
122  
123  
124  
125  
126  
127  
128  
129  
130  
131  
132  
133  
134  
135  
136  
137  
138  
139  
140  
141  
142  
143  
144  
145  
146  
147  
148  
149  
150  
151  
152  
153  
154  
155  
156  
157  
158  
159  
160  
161  
162  
163  
164  
165  
166  
167  
168  
169  
170  
171  
172  
173  
174  
175  
176  
177  
178  
179  
180  
181  
182  
183  
184  
185  
186  
187  
188  
189  
190  
191  
192  
193  
194  
195  
196  
197  
198  
199  
200  
201  
202  
203  
204  
205  
206  
207  
208  
209  
210  
211  
212  
213  
214  
215  
216  
217  
218  
219  
220  
221  
222  
223  
224  
225  
226  
227  
228  
229  
230  
231  
232  
233  
234  
235  
236  
237  
238  
239  
240  
241  
242  
243  
244  
245  
246  
247  
248  
249  
250  
251  
252  
253  
254  
255  
256  
257  
258  
259  
260  
261  
262  
263  
264  
265  
266  
267  
268  
269  
270  
271  
272  
273  
274  
275  
276  
277  
278  
279  
280  
281  
282  
283  
284  
285  
286  
287  
288  
289  
290  
291  
292  
293  
294  
295  
296  
297  
298  
299  
300  
301  
302  
303  
304  
305  
306  
307  
308  
309  
310  
311  
312  
313  
314  
315  
316  
317  
318  
319  
320  
321  
322  
323  
324  
325  
326  
327  
328  
329  
330  
331  
332  
333  
334  
335  
336  
337  
338  
339  
340  
341  
342  
343  
344  
345  
346  
347  
348  
349  
350  
351  
352  
353  
354  
355  
356  
357  
358  
359  
360  
361  
362  
363  
364  
365  
366  
367  
368  
369  
370  
371  
372  
373  
374  
375  
376  
377  
378  
379  
380  
381  
382  
383  
384  
385  
386  
387  
388  
389  
390  
391  
392  
393  
394  
395  
396  
397  
398  
399  
400  
401  
402  
403  
404  
405  
406  
407  
408  
409  
410  
411  
412  
413  
414  
415  
416  
417  
418  
419  
420  
421  
422  
423  
424  
425  
426  
427  
428  
429  
430  
431  
432  
433  
434  
435  
436  
437  
438  
439  
440  
441  
442  
443  
444  
445  
446  
447  
448  
449  
450  
451  
452  
453  
454  
455  
456  
457  
458  
459  
460  
461  
462  
463  
464  
465  
466  
467  
468  
469  
470  
471  
472  
473  
474  
475  
476  
477  
478  
479  
480  
481  
482  
483  
484  
485  
486  
487  
488  
489  
490  
491  
492  
493  
494  
495  
496  
497  
498  
499  
500  
501  
502  
503  
504  
505  
506  
507  
508  
509  
510  
511  
512  
513  
514  
515  
516  
517  
518  
519  
520  
521  
522  
523  
524  
525  
526  
527  
528  
529  
530  
531  
532  
533  
534  
535  
536  
537  
538  
539  
540  
541  
542  
543  
544  
545  
546  
547  
548  
549  
550  
551  
552  
553  
554  
555  
556  
557  
558  
559  
560  
561  
562  
563  
564  
565  
566  
567  
568  
569  
570  
571  
572  
573  
574  
575  
576  
577  
578  
579  
580  
581  
582  
583  
584  
585  
586  
587  
588  
589  
590  
591  
592  
593  
594  
595  
596  
597  
598  
599  
600  
601  
602  
603  
604  
605  
606  
607  
608  
609  
610  
611  
612  
613  
614  
615  
616  
617  
618  
619  
620  
621  
622  
623  
624  
625  
626  
627  
628  
629  
630  
631  
632  
633  
634  
635  
636  
637  
638  
639  
640  
641  
642  
643  
644  
645  
646  
647  
648  
649  
650  
651  
652  
653  
654  
655  
656  
657  
658  
659  
660  
661  
662  
663  
664  
665  
666  
667  
668  
669  
670  
671  
672  
673  
674  
675  
676  
677  
678  
679  
680  
681  
682  
683  
684  
685  
686  
687  
688  
689  
690  
691  
692  
693  
694  
695  
696  
697  
698  
699  
700  
701  
702  
703  
704  
705  
706  
707  
708  
709  
710  
711  
712  
713  
714  
715  
716  
717  
718  
719  
720  
721  
722  
723  
724  
725  
726  
727  
728  
729  
730  
731  
732  
733  
734  
735  
736  
737  
738  
739  
740  
741  
742  
743  
744  
745  
746  
747  
748  
749  
750  
751  
752  
753  
754  
755  
756  
757  
758  
759  
760  
761  
762  
763  
764  
765  
766  
767  
768  
769  
770  
771  
772  
773  
774  
775  
776  
777  
778  
779  
780  
781  
782  
783  
784  
785  
786  
787  
788  
789  
790  
791  
792  
793  
794  
795  
796  
797  
798  
799  
800  
801  
802  
803  
804  
805  
806  
807  
808  
809  
810  
811  
812  
813  
814  
815  
816  
817  
818  
819  
820  
821  
822  
823  
824  
825  
826  
827  
828  
829  
830  
831  
832  
833  
834  
835  
836  
837  
838  
839  
840  
841  
842  
843  
844  
845  
846  
847  
848  
849  
850  
851  
852  
853  
854  
855  
856  
857  
858  
859  
860  
861  
862  
863  
864  
865  
866  
867  
868  
869  
870  
871  
872  
873  
874  
875  
876  
877  
878  
879  
880  
881  
882  
883  
884  
885  
886  
887  
888  
889  
890  
891  
892  
893  
894  
895  
896  
897  
898  
899  
900  
901  
902  
903  
904  
905  
906  
907  
908  
909  
910  
911  
912  
913  
914  
915  
916  
917  
918  
919  
920  
921  
922  
923  
924  
925  
926  
927  
928  
929  
930  
931  
932  
933  
934  
935  
936  
937  
938  
939  
940  
941  
942  
943  
944  
945  
946  
947  
948  
949  
950  
951  
952  
953  
954  
955  
956  
957  
958  
959  
960  
961  
962  
963  
964  
965  
966  
967  
968  
969  
970  
971  
972  
973  
974  
975  
976  
977  
978  
979  
980  
981  
982  
983  
984  
985  
986  
987  
988  
989  
990  
991  
992  
993  
994  
995  
996  
997  
998  
999  
1000

Observed damage to the specimen was minimal. Flexural cracks were detected in the beams, spaced at approximately 250 mm, but closed after testing. No flexural cracks were observed in the column. Up to 2 percent drift, virtually no cracking was observed in the joint region. Some small cracks, approximately 50 mm in length, were observed in the beam corners from the end of the channel’s flange. They formed when this region was in compression from connection opening. Beyond 2% drift, some additional cracks were observed, but were minor. No cracks were observed around the armouring in the column, nor were any diagonal shear cracks observed across the joint. No crushing was observed around the steel armouring the column. Upon the completion of testing, there was a prestress loss of 4% per thread-bar in the East-West and North-South direction.

1  
2  
3  
4  
5  
6  
7  
8  
9  
10  
11  
12  
13  
14  
15  
16  
17  
18  
19  
20  
21  
22  
23  
24  
25  
Results from bi-directional testing are given as individual East-West and North-South direction plots in Figure 6, with the bi-directional clover-leaf displacement-controlled loading pattern shown inset in Figure 6a. The specimen exhibited stable and highly dissipative hysteresis loops with negligible stiffness or strength degradation. The bi-directional rocking caused some additional 50-100mm minor crack propagation to the beams near the joint interface. These cracks appeared when the specimen was displaced concurrently in the East-West and North-South (diagonal) direction, resulting from significant force concentration at the rocking corner of the beams. Comparing the uni- and bi-directional hysteresis loops indicates that the specimen performed essentially the same as in uni-directional loading. Very minor strength loss from the bi-directional testing is noticeable at the 3 percent drift amplitude.

26  
27  
28  
29  
30  
31  
32  
33  
34  
35  
36  
Figure 8 shows the compression force in two of the dampers over time, recorded after quasi-static testing to 3% drift. In the first 8 hours, the initial 200 kN compression force dropped to ~100 kN. After 40 hours, it reduced to ~85kN, following the logarithmic decay in Figure 8.

### 37 38 39 40 41 42 43 44 45 46 47 48 49 50 51 52 53 54 55 **Quasi-earthquake displacement test results**

56  
57  
58  
59  
60  
61  
62  
63  
64  
65  
Figure 9 shows the experimental results for the three IDA selected earthquakes used as QED test inputs. The force-displacement response, the bi-directional column orbit, and the displacement versus time are shown. In all cases, the specimen exhibited good flag-shaped hysteretic energy dissipation response. Bi-directional rocking coupled with non-uniform displacement cycles, resulted in some minor stiffness degradation. This loss is evident when scrutinizing the North-South force-displacement response, particularly for the 50% MCE case which exhibited significant biaxial motion interaction.

Damage to the specimen was minimal with only slight cracking near the joint region observed. These cracks generally closed at the end of testing. Some prestress losses of 0-15 kN were detected, and attributed to a combination of some local cracking/crushing of the

concrete around the thread-bar anchorages, as well as normal tendon-duct frictional effects.

1  
2  
3 **MULTI-LEVEL SEISMIC PERFORMANCE ASSESSMENT**  
4  
5

6 Ground motions representing different levels of seismic demand were applied to a  
7 subassembly representing an exterior column of a multi-storey building. Using these test  
8 results, it is possible to extrapolate observed damage to the whole structure and determine if  
9 identified performance objectives were met. The first deals with serviceability. Given a design  
10 level earthquake, there must be high confidence that the structure will not sustain damage that  
11 disrupts normal function. The seismic demand for this objective is the 90<sup>th</sup> percentile DBE  
12 (10% probability in 50 years/475-year return period). The displacement profile had a single,  
13 large 1.6% interstory drift cycle, followed by a slow reduction in displacement. Residual drift  
14 was negligible. Observed damage from this level of shaking was minimal. Flexural cracks  
15 were observed in the beams and small (50 mm) cracks that closed after testing were observed  
16 in the beam’s joint region. The HF2V dampers performed well, with some hysteretic energy  
17 dissipation on the first pulse, followed by near-elastic behaviour. The specimen did not suffer  
18 any stiffness or strength degradation, as shown in the experimental results of Figure 6, and in  
19 more detail in Rodgers (2009). Given these results, the specimen satisfied the first MSPA  
20 requirement that the building should remain operational following a DBE.  
21  
22  
23  
24  
25  
26  
27  
28  
29  
30  
31  
32  
33  
34  
35  
36  
37  
38  
39  
40  
41

42 The second performance objective relates to repairability, where there must be moderate  
43 confidence the structure is repairable following a rare earthquake. This criteria relates to the  
44 50<sup>th</sup> percentile MCE (2% probability in 50 years/2450 year return period). The displacement  
45 demand was most severe in the North-South (gravity) direction, corresponding to a maximum  
46 interstory drift of 1.6%. Again, the specimen performed very well. Only a few additional  
47 cracks near the beam’s armouring were observed. In the East-West direction, the specimen  
48 behaved elastically, with no stiffness or strength degradation. In the North-South direction,  
49 some minor stiffness degradation was observed, and attributed to binding of the draped  
50  
51  
52  
53  
54  
55  
56  
57  
58  
59  
60  
61  
62  
63  
64  
65

1 thread-bar profile within the duct. The specimen thus easily met the second MSPA  
2 requirement.  
3

4 The final performance objective relates to collapse prevention and life-safety. With a  
5 high level of confidence the structure must not collapse following a very rare earthquake. This  
6 objective was related to the 90<sup>th</sup> percentile MCE. The displacement demand consisted of one  
7 primary pulse to 2.8% East-West interstory drift (3.1% radial drift), followed by several small  
8 cycles. As with the previous two earthquakes, damage to the specimen was minimal. Some  
9 previously developed cracks propagated away from the joint another 100 mm. A few  
10 additional cracks formed near the armouring region, but mostly closed after testing. During  
11 the first pulse, a considerable amount of hysteretic energy dissipation was observed,  
12 subsequent displacement cycles were elastic, with the full stiffness and strength of the  
13 specimen preserved. Some prestress losses were recorded, of ~0-5%, likely due to embedding  
14 in the anchorage regions. These losses were deemed too small to necessitate re-stressing the  
15 thread-bars. Given the damage outcome from this level of demand, the structure satisfied the  
16 final objective of life-safety.  
17  
18  
19  
20  
21  
22  
23  
24  
25  
26  
27  
28  
29  
30  
31  
32  
33  
34

35 It is considered that this dual experimental-computational MSPA has verified the  
36 seismic resistance capability of the proposed structural system with jointed precast concrete  
37 with internal HF2V dampers. The investigation has demonstrated that the specimen, and  
38 indirectly the structure, is capable of remaining essentially damage-free under maximum  
39 considered severe ground shaking conditions. All performance objectives related to  
40 serviceability and life-safety were achieved. This structure, designed to avoid damage by  
41 rocking at specially detailed joints, thus offers an attractive alternative to conventional  
42 monolithic design and construction. The authors believe an equivalent monolithic structure  
43 would have likely undergone severe cyclic rotations at its plastic hinges, resulting in major  
44 damage locally and excessive residual displacement of the global system.  
45  
46  
47  
48  
49  
50  
51  
52  
53  
54  
55  
56  
57  
58  
59  
60  
61  
62  
63  
64  
65

## DISCUSSION

1  
2 Overall, the specimen performed as expected, exhibiting very stable hysteresis loops  
3  
4 with no stiffness or strength degradation and negligible residual drift. Minor cracks were  
5  
6 observed in the joint region of the beam, ranging in length from 25 to 150 mm. These cracks  
7  
8 were confined primarily to the armoured end regions and tended to close after testing. No  
9  
10 damage (cracking or crushing) was observed in the column. This was likely attributed to the  
11  
12 average axial stress ( $\sim 0.1f'_c$ ) in the column that suppressed cracking.  
13  
14  
15

16  
17 Testing confirmed that the detailing strategy is sufficient to protect the members from  
18  
19 damage due to bi-directional drifts up to 4 percent. The joint was shown to 'roll' slightly, but  
20  
21 this effect was minimal. Given the good agreement between the prediction and experimental  
22  
23 results, using the rigid body assumption and the negligible rolling of the connection, the hand  
24  
25 analysis method is demonstrated to be of sufficient sophistication for predicting the backbone  
26  
27 response. The design of the beam-column joint region was relatively simple. However, it is  
28  
29 important to emphasise that checks be made to ensure that armouring is sufficient for  
30  
31 spreading the compressive contact forces to the concrete without damage. Since very little  
32  
33 cracking was observed in the joint region, the steel fibre reinforcing (in the closure pour) did  
34  
35 not play a critical role in the joint's response. It is thus suggested that the addition of fibres to  
36  
37 the mix are not strictly necessary. To further investigate these types of effects, a finite-  
38  
39 element analysis may be necessary to identify any portions which may have been over-  
40  
41 designed.  
42  
43  
44  
45  
46  
47

48  
49 A particular focus of this research was an examination of the efficacy of the internal  
50  
51 HF2V dampers. Results show that the HF2V dampers successfully achieved their design  
52  
53 objectives. The HF2V dampers provided stable energy dissipation, and were shown to 'reset'  
54  
55 after testing, as the residual force in the devices decayed logarithmically. This effect is very  
56  
57 desirable, particularly considering that the devices would not have to be serviced or replaced  
58  
59 following an earthquake.  
60  
61  
62  
63  
64  
65

1 Due to the very small connection opening (~5-10 mm), the effectiveness of the HF2V  
2 damper is very sensitive to its stiffness and connection to the structural system. To limit  
3 stiffness losses from connecting elements the HF2V dampers were tightened against the  
4 connecting rods and the threaded rods grouted in the column. However, some minor slackness  
5 in the connecting elements led to a reduction in stiffness of approximately 60 percent. Further  
6 development of these devices and systems should thus consider connection details.  
7  
8  
9  
10  
11  
12

13 A considerable amount of effort was devoted to identify the most constructible solution  
14 possible. The key to this design is the inclusion of the cast in-situ closure pour. This approach  
15 provides a means of ensuring a reliable contact surface at the joint and easier coupling of  
16 various elements, thus enabling segmental pre-cast construction.  
17  
18  
19  
20  
21  
22

23 The MSPA method relies heavily on the computational model developed from the  
24 experimental data. In order for realistic displacement profiles to be extracted from the model,  
25 the response of the two must be reasonably identical. Furthermore, non-structural damage,  
26 which constitutes a large portion of overall damage, should be considered for a more complete  
27 conclusion to be drawn. Nevertheless, the MSPA method has demonstrated a sound means of  
28 experimentally verifying the performance of structures at various levels of seismic demand.  
29  
30  
31  
32  
33  
34  
35  
36  
37  
38  
39

## 40 **CONCLUSIONS**

41  
42 The following conclusions can be drawn from this study:

- 43 1. The jointed precast concrete specimen with internal HF2V dampers in the beam-end re-  
44 gions satisfied all seismic performance objectives related to serviceability and life-safety.  
45 The specimen remained essentially damage-free, fulfilling the Damage Avoidance Design  
46 objective, after being subjected to displacement profiles representing a design basis earth-  
47 quake and more severe maximum considered earthquakes  
48  
49
- 50 2. The HF2V dampers mounted internally at each beam end provide reliable energy  
51 dissipation on every test cycle. Residual device compression forces were shown to  
52  
53  
54  
55  
56  
57  
58  
59  
60  
61  
62  
63  
64  
65

logarithmically decay through creep towards zero force over time. The devices do not need to be serviced or replaced following an earthquake.

3. The detailing strategy provided an excellent level of protection from damage, while retaining a degree of simplicity and constructability. Throughout quasi-static and QED testing up to 3.1% radial drift the specimen suffered negligible damage; only some small cracks were observed near the steel armouring and these generally closed after testing.

## REFERENCES

- 1  
2  
3 Ajrab, J., Pekcan, G., and Mander, J. (2004). "Rocking Wall–Frame Structures with  
4 Supplemental Tendon Systems." *Journal of Structural Engineering, ASCE*, 130(6), 895-  
5 903.  
6  
7  
8  
9 Baker, J., Cornell, C.A. 2005. A vector-valued ground motion intensity measure consisting of  
10 spectral acceleration and eplison. *Earthquake Engineering and Structural Dynamics*.  
11 **34**(10): 1193-1217.  
12  
13  
14  
15 Bradley, B., Dhakal, R., Mander, J., and Li, L. (2008). "Experimental multi-level seismic  
16 performance assessment of 3D RC frame designed for damage avoidance." *Earthquake*  
17 *Engineering & Structural Dynamics (EESD)*, Vol 37, pp 1-20.  
18  
19  
20  
21  
22 Christopoulos C, Tremblay R, Kim H-J, Lacerte M. (2008) "Self-Centering Energy  
23 Dissipative Bracing System for the Seismic Resistance of Structures: Development and  
24 Validation" *Journal of Structural Engineering – ASCE* **134**(1):96-107 - DOI:  
25 10.1061/(ASCE)0733-9445(2008)134:1(96)  
26  
27  
28  
29  
30 Cousins WJ and Porritt T E. 1993, Improvements to lead-extrusion damper technology.  
31 *Bulletin of the New Zealand National Society for Earthquake Engineering*; **26**:342-348.  
32  
33  
34  
35 Dhakal, R.P. Mander, J.B. Mashiko, N. 2006. Identification of Critical Earthquakes for  
36 Seismic Performance Assessment of Structures, *Earthquake Engineering and Structural*  
37 *Dynamics*; **35**(8):989-1008.  
38  
39  
40  
41  
42 Dolce M, Cardone, D, Ponzo FC, Valente C. (2005) "Shaking table tests on reinforced  
43 concrete frames without and with passive control systems" *Earthquake Engineering and*  
44 *Structural Dynamics*. **34**:1687–1717, DOI: 10.1002/eqe.501  
45  
46  
47  
48  
49 Dutta, A. Mander, J.B. Kokorina, T. 1999. Retrofit for control and reparability of damage.  
50 *Earthquake Spectra*; **15**(4):657-679.  
51  
52  
53  
54 Holden, T., Restrepo, J., and Mander, J. (2003). "Seismic Performance of Precast Reinforced  
55 and Prestressed Concrete Walls." *Journal of Structural Engineering, ASCE*, 129(3), 286-  
56 296.  
57  
58  
59  
60 Li, L., (2006), "Further experiments on the seismic performance of structural concrete beam-



column joints designed in accordance with the principles of damage avoidance”, *Master of Engineering Thesis*. Dept. of Civil Engineering, University of Canterbury, Christchurch, New Zealand. <http://ir.canterbury.ac.nz/handle/10092/1098>

Li, L., Mander, JB, Dhakal, RP, (2008), “Bi-Directional Cyclic Loading Experiment on a 3-D Beam-Column Joint Designed for Damage Avoidance”, *Journal of Structural Engineering*, ASCE, accepted

Mander, J., and Cheng, C.-T. (1997). "Seismic Resistance of Bridges Based on Damage Avoidance Design." *NCEER, Technical Report NCEER-97-0014*, December 10, 1997

Mander, TJ, Rodgers, GW, Chase, JG, Mander, JB, MacRae, GA, Dhakal, RP (2009) “A Damage Avoidance Design Steel Beam-Column Moment Connection Using High-Force-To-Volume Dissipators” *Journal of Structural Engineering*, ASCE, accepted May 09, to appear November 2009.

Pekcan G, Mander JB, Chen SS. (1995) “The Seismic Response of a 1:3 Scale Model R.C. Structure with Elastomeric Spring Dampers” *Earthquake Spectra* **11**(2):249-267

Priestley MJN and Tao JRT. 1993. Seismic Response of Precast Prestressed Concrete Frames with Partially Debonded Tendons. *PCI Journal*, **38**(1):58-69.

Priestley MJN, Sritharan S, Conley JR, Pampanin S. 1999. Preliminary Results and Conclusions from the PRESSS Five-Storey Precast Concrete Test Building. *PCI Journal*, **44**(6):43-67.

Robinson WH, Greenback LR. 1976. An extrusion energy absorber suitable for the protection of structures during an earthquake. *Earthquake Engineering and Structural Dynamics*. **4**:251-259.

Rodgers, GW, Chase, JG, Mander, JB, Leach, NC and Denmead, CS (2007). “Experimental Development, Tradeoff Analysis and Design Implementation of High Force-To-Volume Damping Technology,” *Bulletin of the New Zealand Society of Earthquake Engineering*, Vol 40(2), pp. 35-48

Rodgers, GW, Mander, JB, Chase, JG, Dhakal, RP, Leach, NC, Denmead, CS (2008) "Spectral analysis and design approach for high force-to-volume extrusion damper-based structural energy dissipation" *Earthquake Engineering and Structural Dynamics*, **37**:207-

223.

1  
2 Rodgers, G. W. (2009) "Next Generation Structural Technologies: Implementing High Force-  
3 to-Volume Energy Absorbers" *PhD Thesis*, Dept. of Mechanical Engineering, University of  
4 Canterbury, Christchurch, New Zealand.  
5  
6

7  
8  
9 Shen KL, Soong TT, Chang KC, Lai ML. (1995) "Seismic behaviour of reinforced concrete  
10 frame with added viscoelastic dampers" *Engineering Structures*, **17**(5):372-380.  
11

12  
13 Solberg KM. 2007. Experimental and Financial Investigations into the further development of  
14 Damage Avoidance Design. *Master of Engineering Thesis*. Dept. of Civil Engineering,  
15 University of Canterbury, Christchurch, New Zealand.  
16  
17 <http://ir.canterbury.ac.nz/handle/10092/1162>  
18  
19

20  
21 Sommerville, P, Smith, N, Punyamurthula, S, and Sun, J. "Development of Ground Motion  
22 Time Histories For Phase II Of The FEMA/SAC Steel Project, SAC Background Document  
23 Report SAC/BD-97/04," 1997.  
24  
25

26  
27 Stanton JF, Stone WC, and Cheok GS. 1997. A Hybrid Reinforced Precast Frame for Seismic  
28 Regions. *PCI Journal*, **42**:20-32.  
29  
30

31  
32 Stirling M.W., McVerry G.H., Berryman K.R., 2002 A New Seismic Hazard Model for New  
33 Zealand, *Bulletin of the Seismological Society of America*. **92**(5) pp 1878-1903.  
34  
35

36  
37 Vamvatsikos, D. and Cornell, C.A. 2002. Incremental Dynamic Analysis. *Earthquake*  
38 *Engineering and Structural Dynamics*; **31**:491–514.  
39  
40  
41  
42  
43  
44  
45  
46  
47  
48  
49  
50  
51  
52  
53  
54  
55  
56  
57  
58  
59  
60  
61  
62  
63  
64  
65

1  
2  
3  
4  
5  
6  
7  
8  
9  
10  
11  
12  
13  
14  
15  
16  
17  
18  
19  
20  
21  
22  
23  
24  
25  
26  
27  
28  
29  
30  
31  
32  
33  
34  
35  
36  
37  
38  
39  
40  
41  
42  
43  
44  
45  
46  
47  
48  
49  
50  
51  
52  
53  
54  
55  
56  
57  
58  
59  
60  
61  
62  
63  
64  
65

**Figure 1:** Subassembly development and reinforcing detail

**Figure 2:** Joint region detailing

**Figure 3:** Photographs of the cast in-situ joint showing (a) the east beam with the thread-bar exposed; (b) east beam with the thread-bar enclosed in PVC and showing the damper

**Figure 4:** HF2V Damper details

**Figure 5:** Incremental dynamic analysis curves resulting from the analytical model

**Figure 6:** Uni-directional testing to 3 percent drift: Force-displacement response from experimental testing and the hand method prediction: (a) East-West direction and (b) North-South direction. Inset in a) is the overall clover-leaf pattern resulting from the bidirectional loading

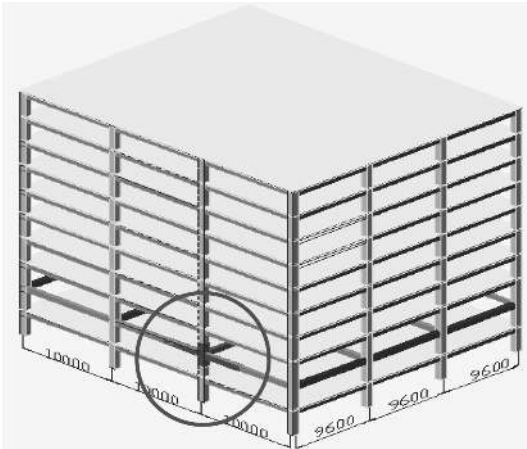
**Figure 7:** Response of (a) the prestress and (b) the ‘in-service’ performance of the HF2V dampers in the east beam.

**Figure 8:** Damper force decay over time. Results are plotted for the east and gravity beam damper. The data is fitted to a logarithmic function.

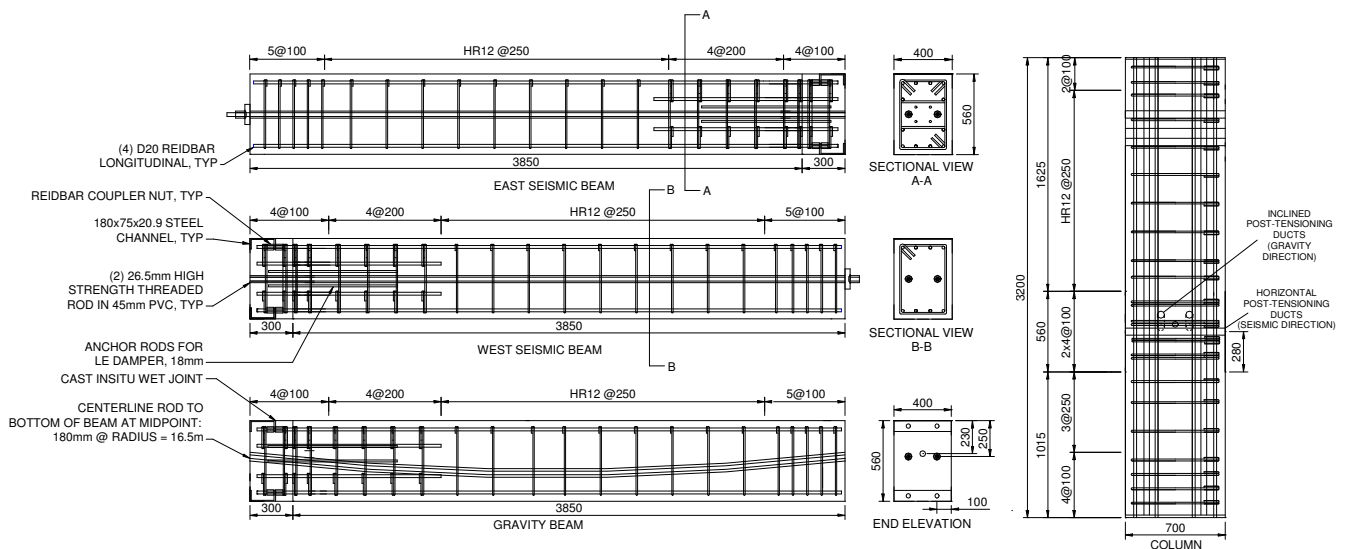
**Figure 9:** QED test results

# Figure

[Click here to download Figure: Figure1.pdf](#)



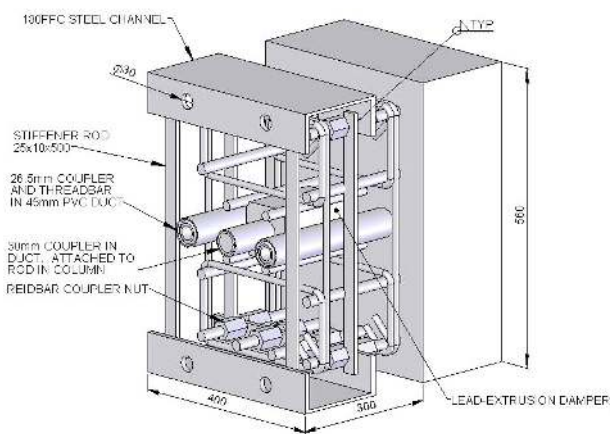
- a) Prototype structure showing the location of subassembly (Solberg, 2007);      b) Photograph of the subassembly in experimental test apparatus



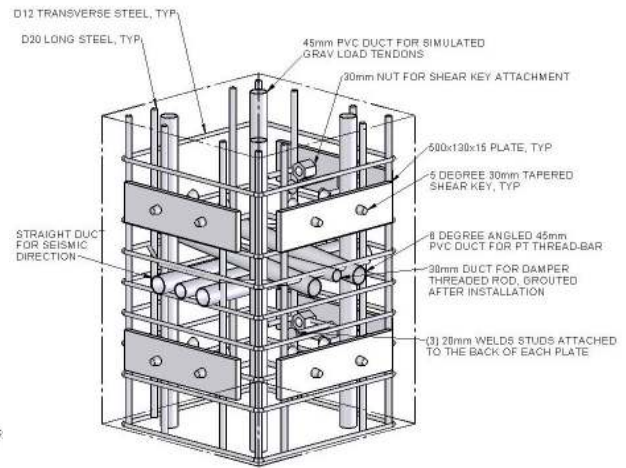
- c) Reinforcing details of the beams and column. Note that the column has horizontal post-tensioning ducts in one direction, and inclined ducts in the orthogonal direction due to draped tendon profile in the gravity beam.

# Figure

[Click here to download Figure: Figure2.pdf](#)



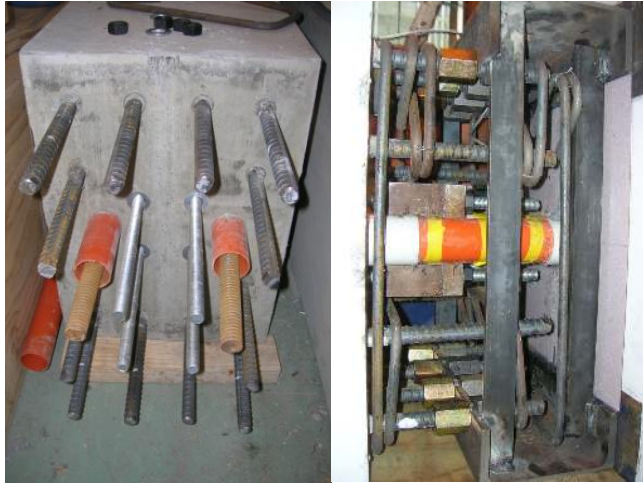
a) Closure pour region at beam end zone



b) Column detailing at the joint region

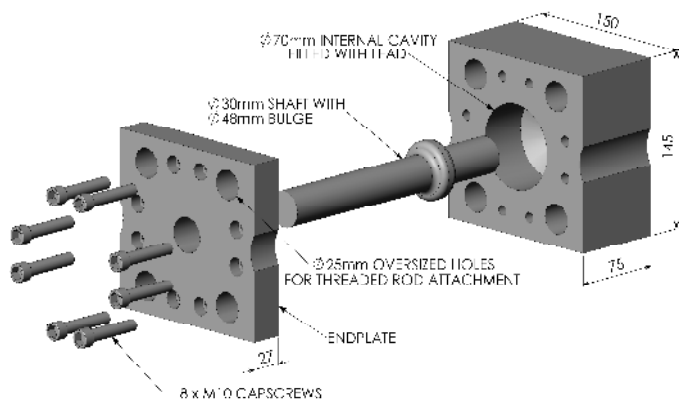
**Figure**

[Click here to download Figure: Figure3.pdf](#)

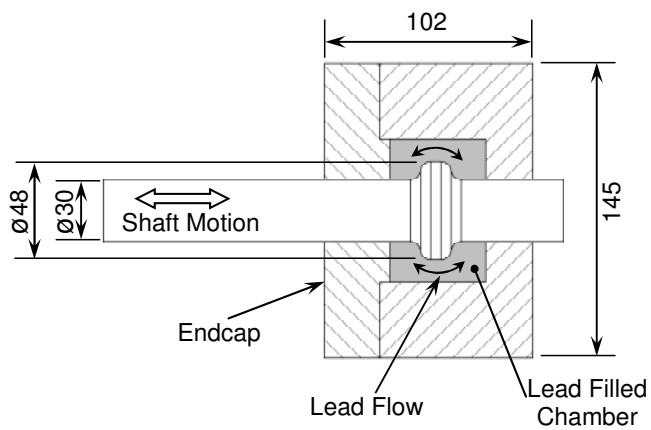


# Figure

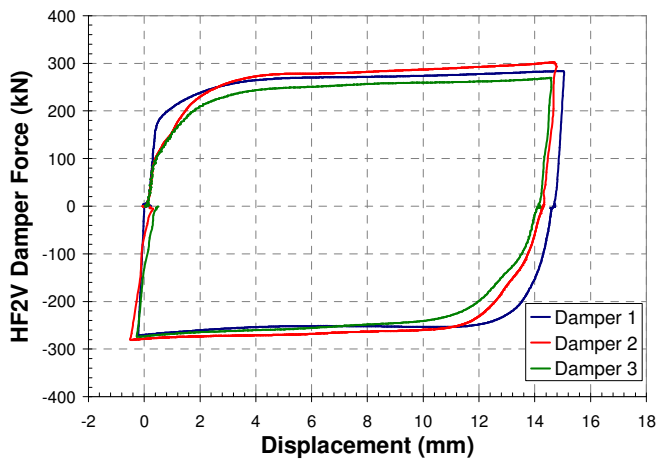
[Click here to download Figure: Figure4.pdf](#)



a) Exploded isometric view

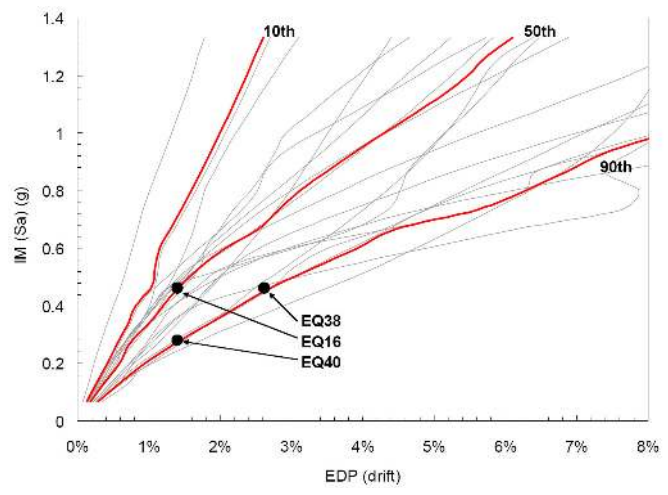


b) Cross-sectional view



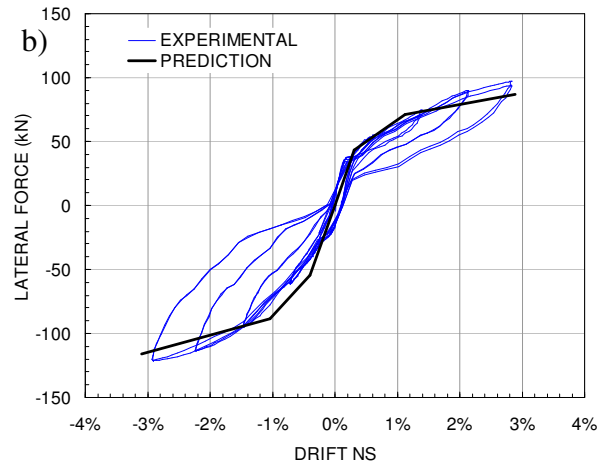
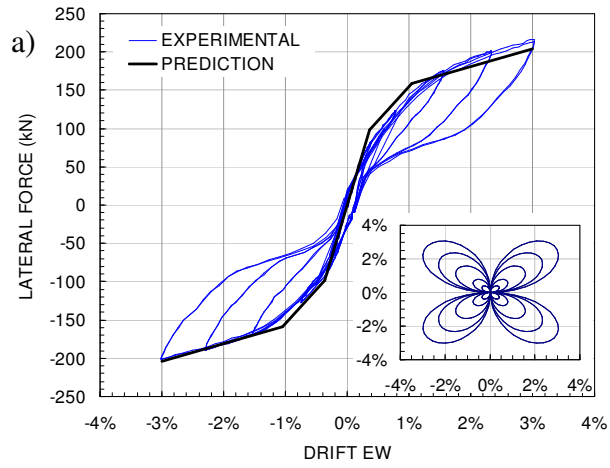
c) Hysteresis loops

Figure  
[Click here to download Figure: Figure5.pdf](#)

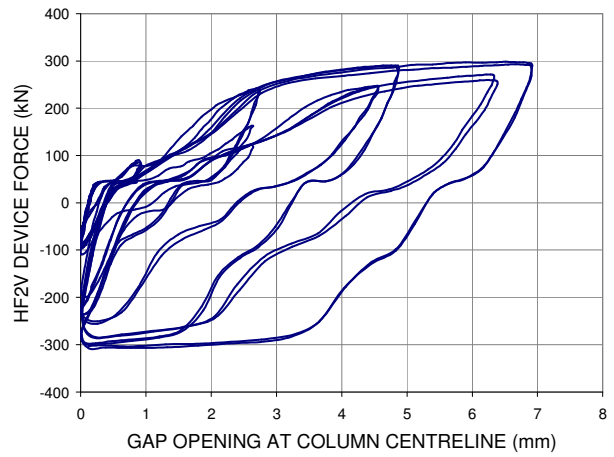
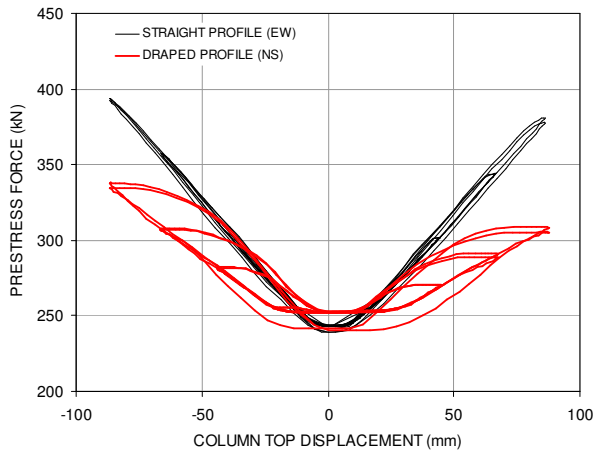




**Figure**  
[Click here to download Figure: Figure6.pdf](#)

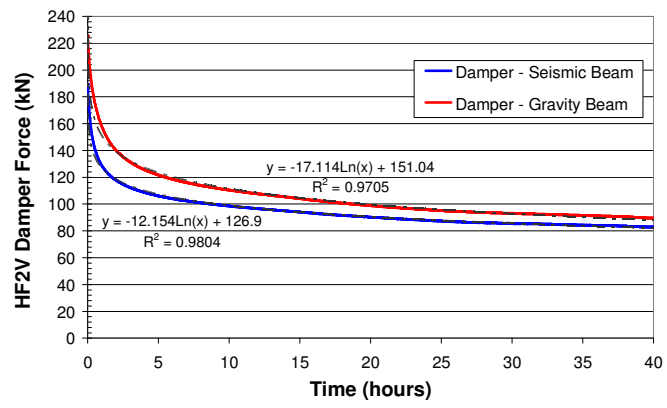


**Figure**  
[Click here to download Figure: Figure7.pdf](#)



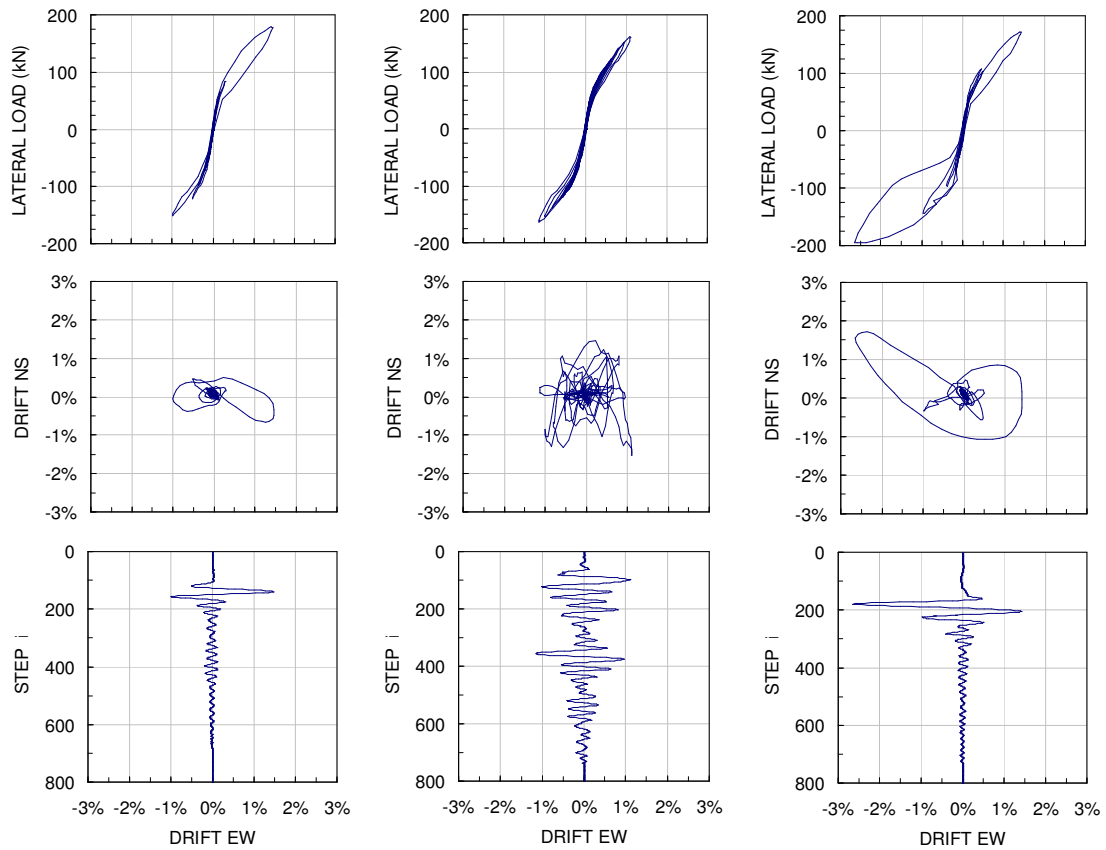
# Figure

[Click here to download Figure: Figure8.pdf](#)

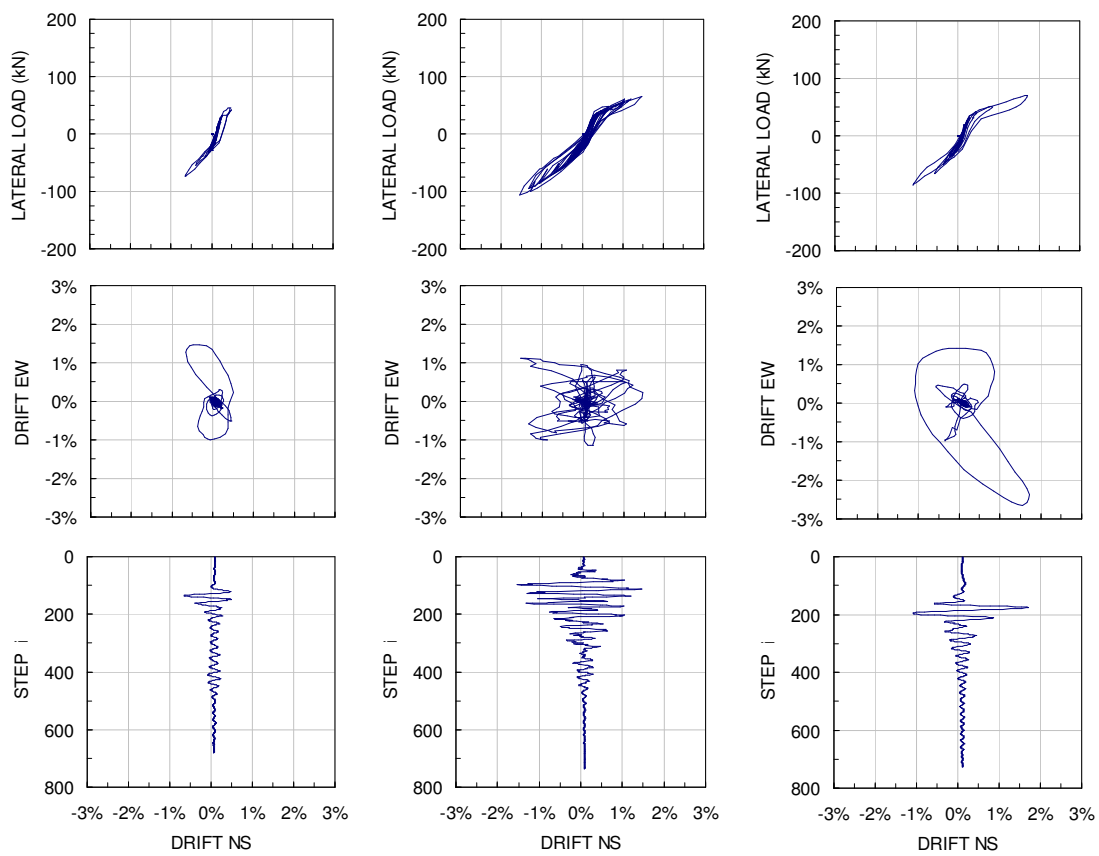


# Figure

[Click here to download Figure: Figure9.pdf](#)



(a) East-West direction results: (left) 90% DBE; (centre) 50% MCE; (right) 90% MCE.



(b) North-South direction results: (left) 90% DBE; (centre) 50% MCE; (right) 90% MCE.



### COPYRIGHT TRANSFER AGREEMENT

Manuscript Number: First Submission - Not yet assigned  
Type: Technical Paper in J. Structural Eng. (ASCE)  
Publication Title: High force to volume seismic dissipaters embedded in concrete frame  
Manuscript Authors: Rodgers, Solberg, Mander, Chase, Bradley, Dhakal  
Corresponding Author Name and Address: Geoffrey Rodgers, c/o Prof J. G. Chase, Dept of Mech. Eng., Univ of Canterbury, Private Bag 4800, Christchurch, New Zealand.


This form *must* be returned with your final manuscript to: American Society of Civil Engineers, Journals Production Services Dept., 1801 Alexander Bell Drive, Reston, VA 20191-4400.

The author(s) warrant(s) that the above cited manuscript is the original work of the author(s) and has never been published in its present form.

The undersigned, with the consent of all authors, hereby transfers, to the extent that there is copyright to be transferred, the exclusive copyright interest in the above-cited manuscript (subsequently called the "work"), in this and all subsequent editions of this work, and in derivatives, translations, or ancillaries, in English and in foreign translations, in all formats and media of expression now known or later developed, including electronic, to the American Society of Civil Engineers subject to the following.

- The undersigned author and all coauthors retain the right to revise, adapt, prepare derivative works, present orally, or distribute the work provided that all such use is for the personal noncommercial benefit of the author(s) and is consistent with any prior contractual agreement between the undersigned and/or coauthors and their employer(s).
- In all instances where the work is prepared as a "work made for hire" for an employer, the employer(s) of the author(s) retain(s) the right to revise, adapt, prepare derivative works, publish, reprint, reproduce, and distribute the work provided that such use is for the promotion of its business enterprise and does not imply the endorsement of ASCE.
- No proprietary right other than copyright is claimed by ASCE.
- An author who is a U.S. Government employee and prepared the above-cited work does not own copyright in it. If at least one of the authors is not in this category, that author should sign below. If all the authors are in this category, check here  and sign here: \_\_\_\_\_ . Please return this form by mail.

SIGN HERE FOR COPYRIGHT TRANSFER [Individual Author or Employer's Authorized Agent (work made for hire)]

Print Author's Name: J. G. Chase Signature of Author (in ink):   
Print Agent's Name and Title: \_\_\_\_\_ Signature of Agency Rep (in ink): \_\_\_\_\_

Date: 3/3/08

Note: If the manuscript is not accepted by ASCE or is withdrawn prior to acceptance by ASCE, this transfer will be null and void and the form will be returned to the author.

\*Failure to return this form will result in the manuscript's not being published.

# ASCE Worksheet for Sizing Technical Papers & Notes

\*\*\*Please complete and save this form then email it with each manuscript submission.\*\*\*

**Note:** The worksheet is designed to automatically calculate the total number of printed pages when published in ASCE format.

<b>Journal Name:</b>	<b>Journal of Structural Engineering</b>	<b>Manuscript # (if known):</b>	<b>STENG-13</b>
<b>Author Full Name:</b>		<b>Author Email:</b>	

The maximum length of a technical paper is 10,000 words and word-equivalents or 8 printed pages. A technical note should not exceed 3,500 word-equivalents in length or 4 printed pages. Approximate the length by using the form below to calculate the total number of words in the text, adding it to the total number of word-equivalents of the figures and tables to obtain a grand total of words for the paper/note to fit ASCE form. Overlength papers must be approved by the editor; however, valuable overlength contributions are not intended to be discouraged by this process.

### 1. Estimating Length of Text

**A. Fill in** the four numbers (highlighted in green) in the column to the right to obtain the total length of text.

**NOTE: Equations take up a lot of space.** Most computer programs don't count the amount of space around display equations. Plan on counting 3 lines of text for every simple equation (single line) and 5 lines for every complicated equation (numerator and denominator).

Estimating Length of Text	
<b>Count # of words in 3 lines of text:</b>	31
Divided by 3	3
Average # of words per line	10
<b>Count # of text lines per page</b>	24
# of words per page	248.00
<b>Count # of pages (don't add references &amp; abstract)</b>	21
Title & Abstract	500
<b>Total # refs</b>	26
Length of Text is	6338
	498
	6836
	6

### 2. Estimating Length of Tables

**A. First count** the longest line in each column across adding two characters between each column and one character between each word to obtain total characters.

1-column table = up to 60 characters wide	2-column table = 61 to 120 characters wide
---	--

**B. Then count** the number of text lines (include footnote & titles)

<b>1-column table = up to 60 characters wide by:</b> 17 lines (or less) = 158 word equiv. up to 34 lines = 315 word equiv. up to 51 lines = 473 word equiv. up to 68 text lines = 630 word equiv.	<b>2-column table = 61 to 120 characters wide by:</b> 17 lines (or less) = 315 word equiv. up to 34 lines = 630 word equiv. up to 51 lines = 945 word equiv. up to 68 text lines = 1260 word equiv.
---	---

**C. Total Characters wide by Total Text lines = word equiv.** as shown in the table above. **Add word equivalents** for each table in the column labeled "Word Equivalents."

### 3. Estimating Length of Figures

**A. First reduce** the figures to final size for publication.

**Figure type size can't be smaller than 6 point (2mm).**

**B. Use ruler** and measure figure to fit 1 or 2 column wide format.

1-column fig. = up to 3.5 in.(88.9mm)	2-col. fig. = 3.5 to 7 in.(88.9 to 177.8 mm) wide
---------------------------------------	---

**C. Then use** a ruler to check the height of each figure (including title & caption).

<b>1-column fig. = up to 3.5 in.(88.9mm) wide by:</b> up to 2.5 in.(63.5mm) high = 158 word equiv. up to 5 in.(127mm) high = 315 word equiv. up to 7 in.(177.8mm) high = 473 word equiv. up to 9 in.(228.6mm) high = 630 word equiv.	<b>2-column fig. = 3.5 to 7 in.(88.9 to 177.8 mm) wide by:</b> up to 2.5 in.(63.5mm) high = 315 word equiv. up to 5 in.(127mm) high = 630 word equiv. up to 7 in.(177.8mm) high = 945 word equiv. up to 9 in.(228.6mm) high = 1260 word equiv.
--	--

**D. Total Characters wide by Total Text lines = word equiv.** as shown in the table above. **Add word equivalents** for each table in the column labeled "Word Equivalents."

Total Tables/Figures:	3994
Total Words of Text:	6836

(word equivalents)

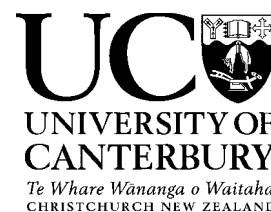
Estimating Length of Tables & Figures		
Tables	Word Equivalents	Figures
Table 1	0	Figure 1
2	0	2
3	0	3
4	0	4
5	0	5
6	0	6
7	0	7
8	0	8
9	0	9
10	0	10
11	0	11
12	0	12
13	0	13
14	0	14
15	0	15
		16
		17
		18
		19
Please double-up tables/figures if additional space is needed (ex. 20+21).		20 and 21

<b>Total words and word equivalents:</b>	<b>10830</b>
<b>printed pages:</b>	<b>9</b>

Department of Mechanical Engineering

University of Canterbury  
Private Bag 4800  
Christchurch

Telephone: +64-3-366 7001  
Facsimile: +64-3-364 2078  
Website: [www.mech.canterbury.ac.nz](http://www.mech.canterbury.ac.nz)



Re: Submission for the Journal of Structural Engineering.

Dear Sir/Madam,

15 July 2009

Please accept our revised article entitled: "*High-Force-To-Volume Seismic Dissipators Embedded In A Jointed Precast Concrete Frame*" by Rodgers et al, for re-review as a full paper to the Journal of Structural Engineering. We found the reviewers comments to be helpful in making the paper stronger.

However, the first reviewer appears to be a practitioner that is either not up to date with emerging DAD literature, as several aspects of this type of design are not well recognised, or simply very interested in the specific construction details. While this interest was well received, the detail requested would fill 2-3 journal articles and does fill two other theses, which are publicly available for download. Hence, we have left some responses to the editor's discretion or relied upon references where space doesn't permit more detail. We ask that the editor bear this in mind when considering the comments of reviewer 1.

All of the comments have been addressed, although some have not been added to the paper on the grounds of length, with reference instead being drawn to other relevant publications where the reader can find the further information. All of the points are addressed in detail for both reviewers on the following pages, although some replies are limited by journal page limits. However, all such cases are explicitly referenced now in the text to provide all necessary supporting material that is not directly relevant to this paper's main focus.

As noted in the sizing worksheet, this paper is marginally over length, with total words and word equivalents now out to 10,830. The authors feel that the paper presents important material in the field and is already very concise, with further reductions in length coming at the cost of important content. We would ask that the editor allow this small extra length in the interests of maintaining the integrity of the current manuscript.

Thank you for your time and effort in this matter. We look forward to your response.

Best Regards,

Mr Geoffrey Rodgers and Prof. J. Geoffrey Chase  
Email: [gwr37@student.canterbury.ac.nz](mailto:gwr37@student.canterbury.ac.nz) and [geoff.chase@canterbury.ac.nz](mailto:geoff.chase@canterbury.ac.nz)  
Phone: 64-3-3642987 x7224

## **Reviewer 1:**

The reviewer's comments are presented here, with the authors' responses.

### **Reviewer 1 writes:**

The paper describes a connection for precast concrete frame members that provides self-centering and energy dissipation. The concept has its origins in work conducted at NIST and in the PRESSS program, but the present development uses a lead extrusion damper in place of yielding mild steel rebars to provide the energy dissipation. The self-centering is provided by prestressing bars that remain elastic during a seismic event.

The concept is an interesting one and appears to be an apt use for the lead extrusion damper, which was first developed in the 1970s but has seen little use in practice (outside New Zealand). The primary advantage offered by the lead is that it creeps, thereby allowing any residual force in the damper after an earthquake to dissipate over time. This is not true of the rebar system. My major overall concern is that the system described here looks too complicated, too congested, too difficult to connect in view of typical on-site tolerances, and too expensive to attract much positive attention from contractors. Therefore it seems unlikely to be implemented, at least in the US. However that is a matter for the marketplace, not reviewers, to determine, so this review will focus on the technical aspects of the paper.

First, placement of the damper at mid-height, rather than at the top and bottom, of the beam means that the displacements imposed on it are relatively small, so the force needs to be correspondingly high if sufficient energy is to be dissipated. That in turn means that the damper needs to have a low yield displacement and that the connecting elements (bolts, rods, etc) must be stiff enough to not isolate the damper by stretching elastically. This is quite a severe requirement, but Figure 4b shows the damper to have a yield displacement of about 1 mm, and the connection tests appeared to show adequate damping. So, although it seems surprising, that concern appears to have been successfully addressed.

Several aspects of the system are difficult to understand from the paper, and the explanations of them should be improved. The primary ones are:

1. The prototype system is unclear. Figure 1a shows the prototype, but what are the beam cross-section dimensions? (the proportions of the test beams are very slender compared with the beams normally used in the US. Slender beams typically lead to joint shear problems). The specified column ties (at 250 mm centers in the test beam, so presumably much larger - and atypical for practice - spacing in the prototype) suggest suspiciously low column shear forces.

- The beam cross-section dimensions of the experimental specimen are presented in Figure 1c. The prototype is scaled for 80% of full-scale, with more details of the prototype structure being discussed in the theses of Li (2006) and Solberg (2007), which is available free on the University of Canterbury institutional repository.

A detailed discussion of the specimen design considerations is not included in this paper, as it focussed on the overall concept and the use of HF2V devices embedded in a damage-avoidance connection.



The sentence on page 5 of the manuscript which originally read:

*“Figure 1b shows the experimental setup, further details of which may be found in Bradley et al (2008).”*

Has been modified to:

*“Figure 1b shows the experimental setup, where further details on the specimen dimensions and design details may be found in Solberg (2007), Bradley et al (2008), and Li (2006).”*

Also, how is the corner column joint detailed? There appears to be little space available for dampers in two orthogonal directions. Does that mean that the system can be used only in "interior bays" of the perimeter, because that would mean only one bay in each direction of the prototype building shown? That seems hardly enough. Or are the interior frames (i.e. the ones spanning between columns in the interior of the building) used for seismic resistance as well? That would be a significant departure from present practice, largely from the point of view of headroom required and the limitations on interior beam depth.

- The experimental subassembly has dampers located in both orthogonal directions (in both the seismic and gravity beams). The only conflicting space constraints are in the column, where the only elements that relate to the dampers are anchor rods. To avoid any interference, a vertical offset of 50mm was provided for the anchor rods that connect the dampers in the gravity beam. Therefore, in the overall building, dampers can be positioned in both the interior and exterior bays of the structure as desired. No clash will be present, and conventional present practice can be maintained.

To better convey this concept to readers, the following sentence on page 6 which originally read:

*“The joint was designed to accommodate 150 x 150 mm HF2V devices in the centre of the joint in the seismic beams, and at a 50 mm offset from centreline in the gravity beam.”*

Has been modified to:

*“The joint was designed to accommodate 150 x 150 mm HF2V devices at mid-height in the beam end-zone in the seismic beams, and at a 50mm vertical offset from mid-height in the gravity beam. This offset prevents any interference between the damper anchor rods from the two orthogonal directions in the column..”*

Is the beam shear really to be carried by the small pins shown in Fig 2b? Not only does that contradict the statement on page 4 that other system need "special key devices" - with the implication that that the proposed system is better because it does not - but they also look like a tolerance nightmare. These matters need to be cleared up, and perhaps the authors would also like to consider stating what the seismic forces on the building and in each beam are, to help the reader understand how the system works. At present, it is hard to evaluate.

- As the reviewer states in the subsequent question 3, the beam shear can be carried in friction at the beam-column interface. However, the shear keys are provided as an additional mechanism to provide some redundancy to the system. The tolerances are not a problem, as the cast-in-situ section at the beam ends allows for adjustment of the steel channels that provide armouring.
- The authors acknowledge that these statements may be debatable. Therefore, the statements the reviewer identifies are modified. The first paragraph in the ‘Subassembly Development’ on page 4, which originally read:

*“Special attention was given to potential construction issues. The beam and column elements were designed to be precast, with limited concrete placement required on-site. Fully precast members require very tight (and costly) tolerances and special shear-key devices to lock the beam to the columns. To avoid this issue, a cast in-situ ‘closure pour’ was provided at one end of each beam. The other end was considered to be a “dry-joint”. Hence: (i) tolerances could be considerably less than fully precast members; (ii) the closure pour provides an access point for coupling the prestress thread-bars and the damping devices; and (iii) high performance concrete can be used in the high stress zone at the beam end. The closure pour thus becomes the primary focus for on-site erection. Within this region, the HF2V damper in each beam can be coupled to a threaded rod anchored in the column, the prestress thread-bars would be coupled to one another, and the channels would be tightened against the face of the column. A detailed overview of the construction sequence is given in Solberg (2007).”*

Has been modified to:

*“Special attention was given to potential construction issues. The beam and column elements were designed to be precast, with limited concrete placement required on-site. A cast in-situ ‘closure pour’ was provided at one end of each beam. The other end was considered to be a “dry-joint”. Hence: (i) tolerances could be less than fully precast members; (ii) the closure pour provides an access point for coupling the prestress thread-bars and the damping devices; and (iii) high performance concrete can be used in the high stress zone at the beam end. The closure pour thus becomes the primary focus for on-site erection. Within this region, the HF2V damper in each beam can be coupled to a threaded rod anchored in the column, the prestress thread-bars would be coupled to one another, and the channels would be tightened against the face of the column. A detailed overview of the construction sequence is given in Solberg (2007).”*

2. Test specimens. Each test beam is said to represent half a real beam. Why then is the tendon in the gravity beam draped so it has the same eccentricity at each end and a low point in the middle (Fig 1c)? It looks like a complete beam.

→ The reviewer is correct that the drape represents a full-beam profile and is in error here. As such, the following modification to the manuscript has been made:

The start of ‘Specimen Design’ on page 5, which originally read:

*“A 3D subassembly representing an interior joint on a lower floor of a ten storey building was developed. The subassembly consisted of two beams cut at their midpoints and an orthogonal beam cut at its midpoint, the approximate location of the point of contraflexure for seismic loads. These beams were all connected to a central column. The orthogonal beam, referred to as the gravity beam, was designed to support one-way precast flooring.”*

Has been modified to:

*“A 3D subassembly representing an interior joint on a lower floor of a ten storey building was developed. The subassembly consisted of two beams cut at their midpoints, the approximate location of the point of contraflexure for seismic loads, and an orthogonal beam designed for gravity loads. These beams were all connected to a central column. The orthogonal beam, referred to as the gravity beam, was designed to support one-way precast flooring.”*

Why also is the steel channel etc. in the beam end needed? (And what is a PFC channel?) It does not appear to connect the damper or the PT bars, but adds to congestion in the end and causes the need for Reidbars (presumably a local equivalent of a threaded Dywidag bar) in the top and bottom of the beam, even though they are not continuous into the column. It would also make casting the c.i.p. closing pour very difficult.

→ The steel channel is required for armouring of the joint region. As noted, it is not connected to either the dampers or PT bars, nor is it continuous into the column. These channels exist for the purpose of providing an armoured rocking interface, whereby the large point loads at the rocking edge is mechanically developed into beam. They also provide an ability to correct any misalignment by the locating nuts on the Reidbars (which are indeed an alternative to Dywidag bars). This is an essential part of the damage avoidance design and is one of the key reasons that no notable stiffness or strength degradation was observed in the experiments. The space is a little limited for the cast in place closure pour, but the gap is sufficient, if not ample, for the final pour.

Regarding the reference to the 180 PFC channel. The reviewer correctly notes that this is not clear, and should be explained to readers. Therefore, the manuscript is modified, where the sentence near the end of page 6, which originally read:

*“A 180 PFC channel was used top and bottom to armour the contact surfaces and was designed to prevent crushing of the concrete behind the channel from compression forces at the design moment of the joint.”*

Has been modified to:

*“A 180mm parallel flange channel (PFC) was used top and bottom to armour the contact surfaces and was designed to prevent crushing of the concrete behind the channel from compression forces at the design moment of the joint.”*

The ties in the column joint are shown (Fig 1c) clashing with something that looks like the damper. Since the region appears to be very congested, demonstrating the adequacy of the space available is important and clashes are unacceptable. Furthermore the ties shown in Fig 1c are different from those shown in Fig 2b. Which figure should the reader believe?

- The authors' would like to reaffirm and clarify that the dampers are not located in the column, but rather in the beam ends. Therefore, the dampers do not clash with the column ties. The dashed hidden-detail lines shown on the column in Figure 1c are the exit points of the tendon ducts on the far face and the trajectory through the column. The solid circles represent the entry points on the front face of the column. Although the tendons do pass through the level of the column ties, they do so at the column centre (not at the tie location) and no clashes exist. It should be noted that the tendon ducts seen in Figure 1c are for the gravity direction with an 8° incline for the draped profile, and are the shown in Figure 2b. The reviewer seems to be confusing the ducts with the horizontal ducts for the seismic direction in Figure 2b, with the gravity direction ducts in Figure 1c.

In Fig 1c, the bottom beam lacks a section callout mark, and the section should be lined up with the elevation view. Why are the east and west seismic beams both shown? They appear to be identical. Showing both suggests that they are not. The gravity beam appears to use PT bars for the draped prestressing (the figure refers to a "rod" and page 17 refers to "the draped threadbar profile"). How are bars used on a curved profile?

- The end elevation of the bottom beam in Figure 1c has no corresponding section callout as it is an end elevation and not a section view. However, the authors acknowledge that greater clarity should be provided to readers to convey this concept. Moreover, both the East and West seismic beams are presented so that different section views can be presented. The authors' agree that the current layout might be a little misleading and have therefore made the following changes to the manuscript.

The end elevation and sectional views are more clearly labelled for greater clarity. The reference to Figure 1c in the text is also modified to convey that both seismic beams are identical, and are reproduced to allow additional detail views.

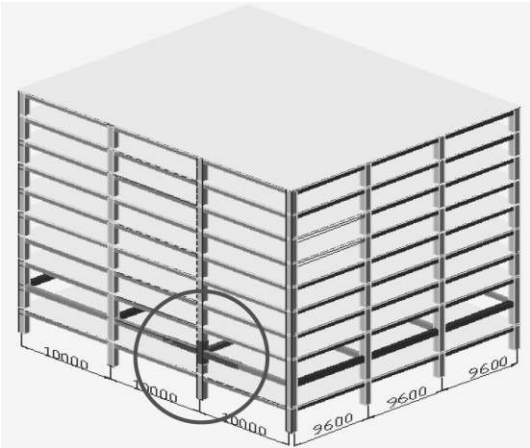
The sentence on page 5 which originally read:

*“Figure 1c illustrates the reinforcing layout for the structural members, where the target longitudinal reinforcement ratio is 0.01.”*

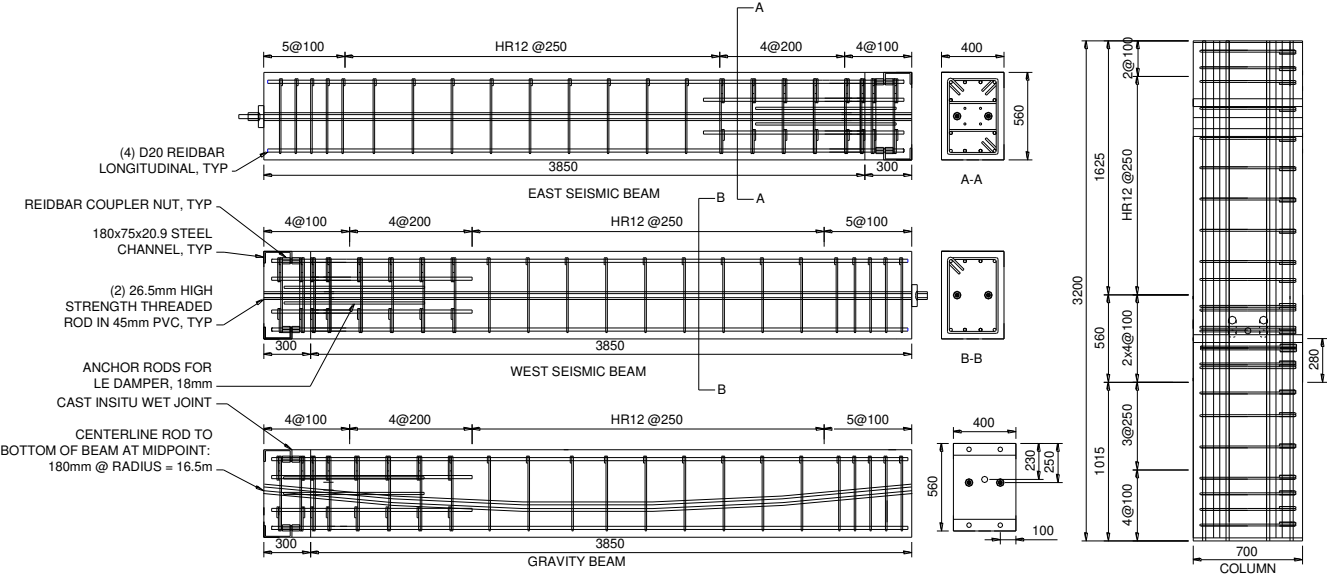
Has been appended and now reads:

*“Figure 1c illustrates the reinforcing layout for the structural members, where the target longitudinal reinforcement ratio is 0.01. Note that in Figure 1c both the seismic beams are shown. These beams are identical, but both are shown to provide additional section views.”*

Figure 1, which originally took the form:



a) Prototype structure showing the location of subassembly (Solberg, 2007);      b) Photograph of the subassembly in experimental test apparatus



c) Reinforcing details of the beams and column

**Figure 1: Subassembly development and reinforcing detail**



3. Under "Construction Considerations" on page 4, the authors claim that "fully precast members require very tight and costly tolerances and special key devices to lock the beams into the columns". These statements are simply not true. Most of the "Hybrid Frames" in the US have been built by Charles Pankow Builders. They have never used any special key devices, because friction holds the beams up. They have never had any trouble erecting the beams, using only a gap at each end of about an inch, which is subsequently grouted. The statement appears designed to suggest false disadvantages for others, so the proposed system looks better.

→ The authors acknowledge that these statements may be debatable. Therefore, the statements the reviewer identifies are modified. The first paragraph in the 'Subassembly Development' on page 4, which originally read:

*“Special attention was given to potential construction issues. The beam and column elements were designed to be precast, with limited concrete placement required on-site. Fully precast members require very tight (and costly) tolerances and special shear-key devices to lock the beam to the columns. To avoid this issue, a cast in-situ ‘closure pour’ was provided at one end of each beam. The other end was considered to be a “dry-joint”. Hence: (i) tolerances could be considerably less than fully precast members; (ii) the closure pour provides an access point for coupling the prestress thread-bars and the damping devices; and (iii) high performance concrete can be used in the high stress zone at the beam end. The closure pour thus becomes the primary focus for on-site erection. Within this region, the HF2V damper in each beam can be coupled to a threaded rod anchored in the column, the prestress thread-bars would be coupled to one another, and the channels would be tightened against the face of the column. A detailed overview of the construction sequence is given in Solberg (2007).”*

Has been modified to:

*“Special attention was given to potential construction issues. The beam and column elements were designed to be precast, with limited concrete placement required on-site. A cast in-situ ‘closure pour’ was provided at one end of each beam. The other end was considered to be a “dry-joint”. Hence: (i) tolerances could be less than fully precast members; (ii) the closure pour provides an access point for coupling the prestress thread-bars and the damping devices; and (iii) high performance concrete can be used in the high stress zone at the beam end. The closure pour thus becomes the primary focus for on-site erection. Within this region, the HF2V damper in each beam can be coupled to a threaded rod anchored in the column, the prestress thread-bars would be coupled to one another, and the channels would be tightened against the face of the column. A detailed overview of the construction sequence is given in Solberg (2007).”*

The proposed system requires mechanical connections to be made at each end. While it is possible to see, at least in theory, how this could be done at the end with the c.i.p. closure pour, it is not clear how this is to be done at the other end, where it seems that the connection is precast-to-precast. (The text says that a closure pour was provided at one end of the beam.

Does this mean at only one end in the prototype? Or is it at both ends in the prototype, but only the one connected end in the test beam?)

- The concept of one precast-to-precast interface and one c.i.p closure pour was to allow for overall tolerances on beam length. One end could be precast with sufficiently tight tolerances so that it can interface with the column, and the other done as a c.i.p closure pour to accommodate variation in beam length. All of the beam-column interfaces in the experimental specimen were cast-in-place, but the overall implementation in a structure would use pre-cast to pre-cast interface at one end and cast-in-place at the other.

The damper connections could be made prior to the off-site fabrication of the beams, and the final connection is only a matter of connecting a threaded rod into a coupler that is connected to the damper. The anchor rod can then be grouted in the column via some existing grout tubes.

While the paper length does not present opportunity to cover these issues in depth, Solberg (2007) is publicly available and referenced to cover this topic that is not the primary focus of this specific article. This thesis can be publicly viewed and downloaded at the University of Canterbury institutional repository at:

<http://ir.canterbury.ac.nz/handle/10092/1162>

4. The configuration of the damper is unclear. First, in Fig. 4a, there are some bolts floating around apparently inside the closure plate. What are they for? Are they in fact the closure plate bolts, but shown in the wrong place? There is a callout to a 70 mm "damper shaft", which looks more like a cavity, because there is already another callout to a 30 mm "damper shaft". What is the 70 mm one? Where does the lead go? It is not shown. If the 70 mm device is indeed a cavity, is it closed at the right hand side as shown? A section would help the reader to understand how the damper works, and in particular the flow path of the lead. The text also mentions a duct that surrounds the damper. Where is it? It is not shown in the figures.

- The reviewer is quite correct in that the exploded view of the device is misleading. The bolts shown are indeed those for the closure plate and are shown in an inappropriate order. The exploded view has been corrected to reflect this comment and the authors would like to thank the reviewer for this comment. Likewise the damper cavity is incorrectly labelled. The cavity is subsequently relabelled.

The authors agree that a sectional view of the damper will be of use to readers and better help convey the damper concept. The addition of a cross-sectional view was originally omitted due to the tight page limit for this journal. In this revision a cross-sectional view is included in addition to the exploded view.

Finally, the damper ducts reference is actually to a duct that contains the damper shaft and connecting rods. The damper duct within the column is grouted to constrain the anchoring rods, and left open within the beam ends to allow the damper shaft to move. The paragraph on page 7/8, which originally read:

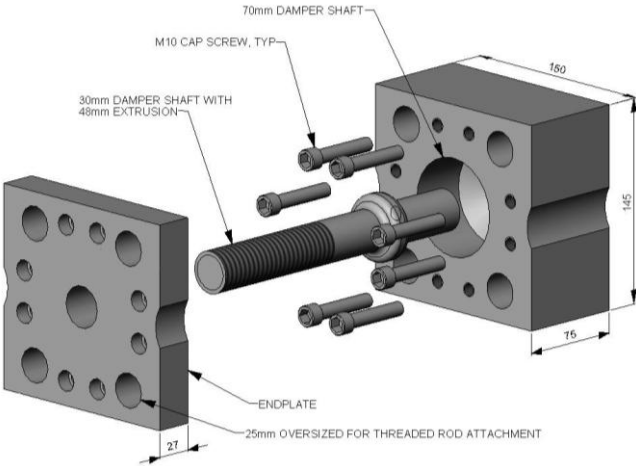


“The column longitudinal reinforcement was welded to a 20 mm steel plate at the top and bottom, and the armouring plates were developed into the concrete by welds studs. A 50 mm recess at the column anchoring ends of the damper duct allowed easy bolt clearance. Corrugated steel tubing provided the damper ducts, with grout tubes at each end.”

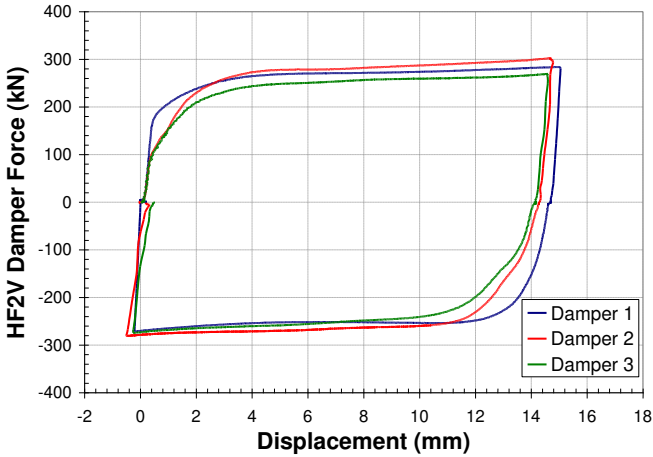
Has been modified to:

“The column longitudinal reinforcement was welded to a 20 mm steel plate at the top and bottom, and the armouring plates were developed into the concrete by welds studs. A 50mm recess at the column face where the damper anchoring rods are bolted allowed easy bolt clearance. Corrugated steel tubing provided the damper ducts where the shaft and connecting rods passed through. Grout tubes are provided to grout the anchoring rod within the column, and the damper duct in the beam ends was left open to allow free movement of the damper shaft.”

Figure 4, which originally took the form:



a) Exploded isometric view



b) Hysteresis loops

**Figure 4: HF2V Damper details**

Has been modified to (now in a column format):

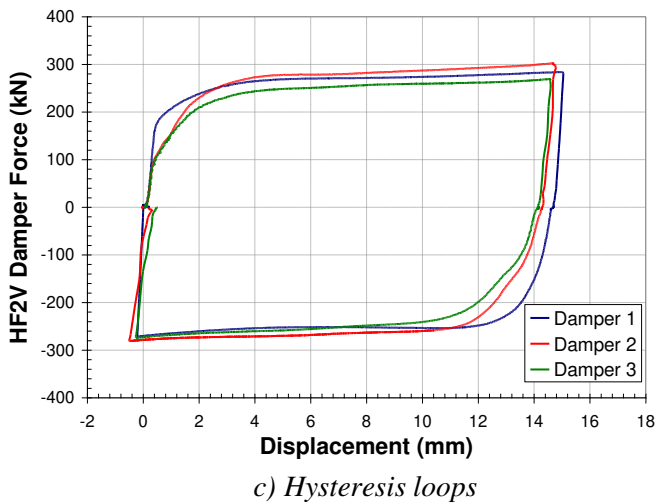
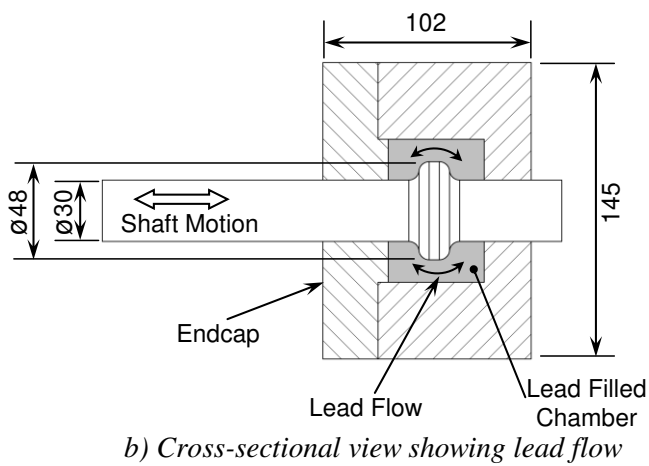
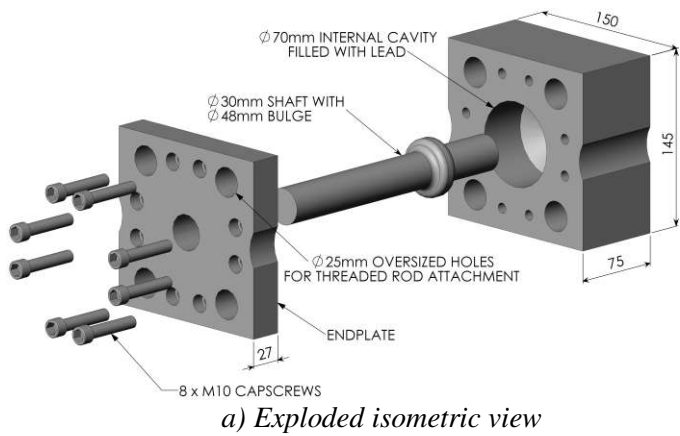


**Figure 4:** HF2V Damper detail

**The inclusion of the exploded view is partially redundant with the addition of the cross-sectional view. However, the authors have included both views in the interests of clarity to the reader. The inclusion of both views is left to the reviewer and editor's discretion based on total paper length**

5. In the section "Predicted Response", the authors refer on page 10 to moment curvature analysis, from which force-displacement response can be calculated. To do this, a plastic hinge length (or something similar) is needed. What was used and with what justification?

- The response prediction assumes elastic behaviour of the structural members and rigid-body deflection. The detailed derivation relates to moment-area methods and simple beam-bending theory. The derivation in the manuscript does not require a plastic hinge length as the members will remain elastic. Full derivation of Equation (8) can be found in the theses of Li (2006) and Rodgers (2009). To reflect this, the following modification has been made to the paper:

On page 10, where it originally read:

*“Given a moment-curvature analysis, the force-displacement response of the subassembly can be evaluated. In the East-West direction, the horizontal force at the top of the column,  $V_{cob}$ , can be found given the moment at the joint.”*

It now reads:

*“Given an elastic moment-curvature analysis, the force-displacement response of the subassembly can be evaluated. In the East-West direction, the horizontal force at the top of the column,  $V_{cob}$ , can be found given the moment at the joint.”*

Moreover, immediately following Equation (8), reference has been drawn to the two theses of Solberg (2007) and Rodgers (2009) to provide additional information to interested readers. Both of these theses will be publicly available on the institutional repository for the University of Canterbury:

Li (2006): <http://ir.canterbury.ac.nz/handle/10092/1098>

Rodgers (2009) is not currently available, but will be in the very near future, and certainly before the final manuscript is published.

6. The "Experimental setup" section was hard to understand without a figure of the setup used. Reference to the "south face of the column" is unhelpful unless the reader is told the orientation of the setup.

- The authors agree that an overall schematic of the experimental setup would be a desired addition to the paper and provide greater clarity to readers. The figure was originally included in the manuscript, but it was removed due to the tight word/word equivalent limit for this journal. Instead reference is drawn to Bradley et al (2008), where a detailed schematic is presented. On page 5 of the manuscript it states:

*“Figure 1b shows the experimental setup, further details of which may be found in Bradley et al (2008).”*

However, the authors do acknowledge that the passage the review makes reference does need to be clearer in the absence of this figure, therefore, the passage on page 11 which originally read:

*“Actuators A and B were located at the top of the east and south face of the column, respectively. Actuator C was orthogonal to the west face of the gravity beam, in line with the gravity beam support strut, and was used primarily to stabilize the specimen.”*

Now reads:

*“Actuators A and B were located at the top of the east and south face of the column, inducing displacements in the seismic and gravity directions, respectively. Actuator C was orthogonal to the side face of the gravity beam, in line with the gravity beam support strut, and was used primarily to stabilize the specimen.”*

**The additional of the following figure would provide further clarity to readers, but will lead to the paper being significantly beyond the word/word equivalent limit. It can be included in full or in part at the reviewers/editors discretion. Otherwise, we feel that the references provided cover these details, as noted in the text, in depth, and they are not a major focus of this paper.**

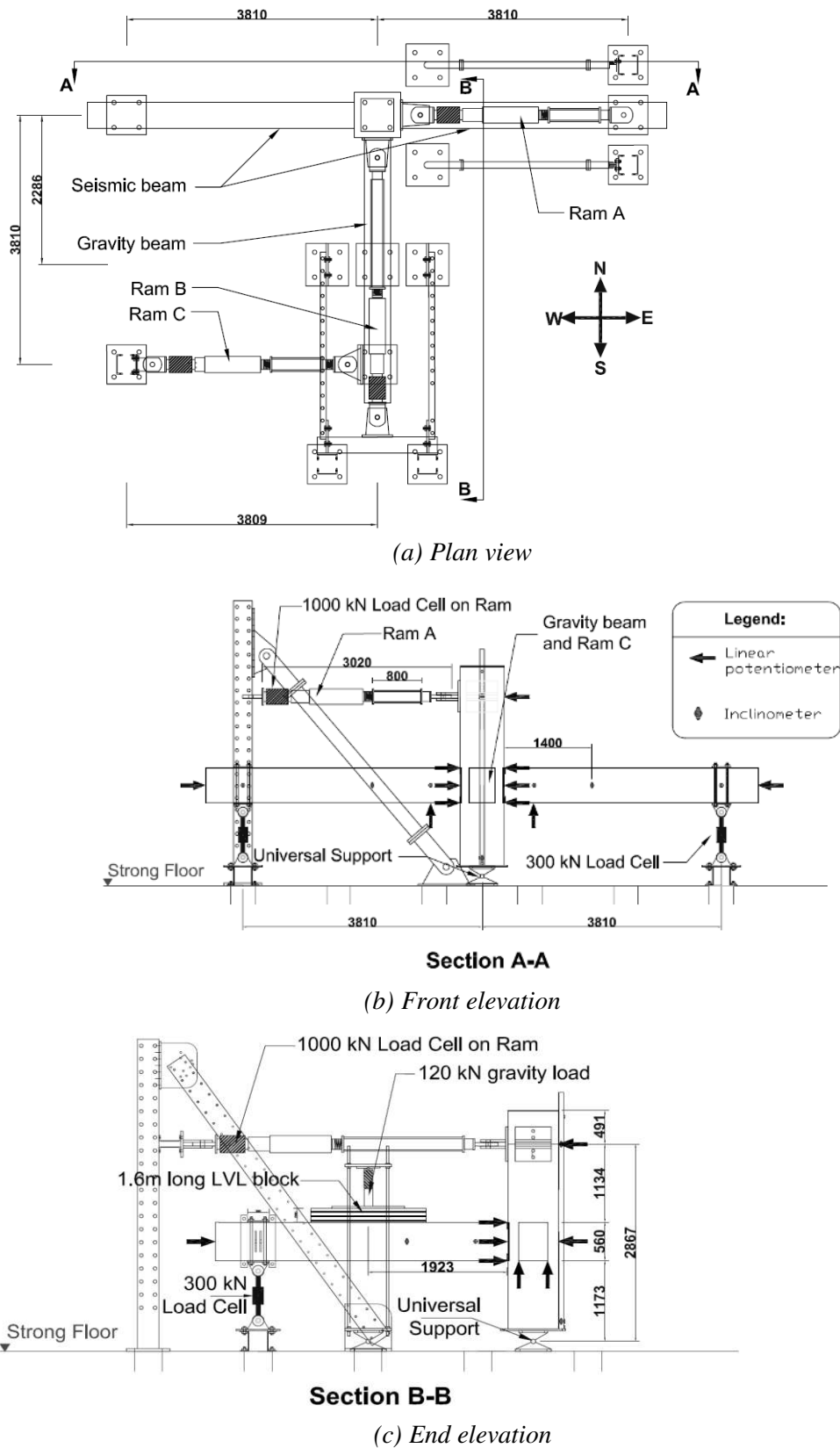


**Figure XX:** Schematic diagrams of the Experimental setup showing actuators and instrumentation

7. Under "Test Methods", oblique references are made to the ground motions used for loading. It would be helpful to know more about them. Reference is also made to an "equivalent computational model". What is that?

- The ground motion used in this study were from the SAC project. The specific details of the ground motions can be found in the new reference provided in the last paragraph of the 'Test Methods' section, on page 14. This reference details the development of the suite of ground motions. The derivation of the ground motion was considered to be outside the scope of this manuscript, as it is already at the page limit. The tight page limit of this journal does not currently allow for additional information about such aspects.

The new reference is:

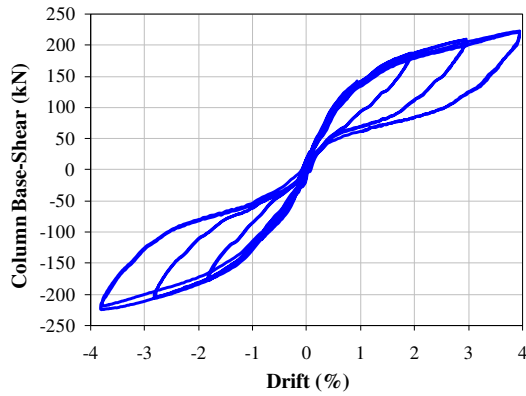
*Sommerville, P, Smith, N, Punyamurthula, S, and Sun, J. "Development of Ground Motion Time Histories For Phase II Of The FEMA/SAC Steel Project, SAC Background Document Report SAC/BD-97/04," 1997.*

Regarding the computational model. Detailed description of the model is not the focus of this paper, and cannot be included within the tight page limit. An earlier draft of this paper included details of the model, but was removed due to the page limit. Instead, reference is drawn to the thesis of Solberg (2007) in the 'Test Methods' section on page 12, which details the equivalent computational model.

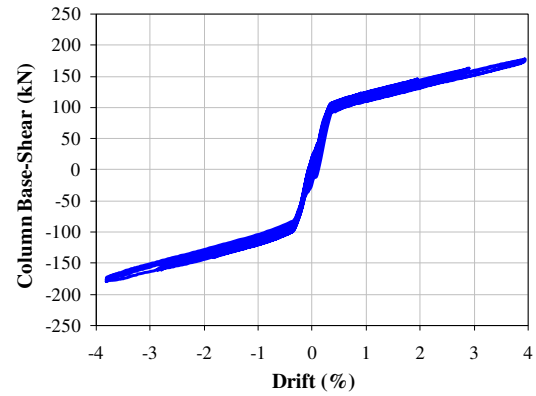
8. "Experimental Results". The text claims that the results shown in Figure 6 are "highly dissipative". That is a value judgment and, by the look of the rather skinny hysteresis loops, one with which many engineers would not agree. Some better explanation is needed.

- The statement of "highly dissipative" was made in the context of damage-avoidance design structures. More specifically, as the structural members remain elastic, they provide essentially no dissipation, and the straight tendon profile results in very little inherent dissipation for the connection without dampers. Therefore, the authors feel that the hysteresis loops presented in Figure 6 are highly dissipative given that no structural damage occurs.

Following the testing regime presented within this manuscript, the damper connecting rods were cut to remove the damper contributions to the connection response. Without the damper contributions the inherent energy dissipation of the connection is very low. The following figure shows a comparison of the joint hysteresis with and without dampers under uni-directional loading in the East-West (seismic) direction to 4% drift.



a) 500 kN total prestress, with dampers



b) 500 kN total prestress, without dampers

→ The authors acknowledge that, despite the reasoning presented above, these results are not presented in the manuscript, and therefore cannot be used to justify the statement in question. While the comparison of subassembly performance with and without damper contributions is an important consideration, length restriction prevent these results being presented.

**If the reviewer feels that these results should be included in the manuscript, then they can be added at the editor's discretion.**

As a compromise, the authors' have modified the manuscript to describe the reasoning presented above using only text. The statement questioned by the reviewer on page 14 of the original manuscript which originally read:

*“In the EW direction, highly dissipative hysteretic behaviour is apparent. The specimen did not suffer any noticeable stiffness or strength degradation, and stable hysteretic energy dissipation is evident.”*

Has been modified to reflect this reasoning:

*“In the East-West direction, the hysteretic behaviour displays notable energy dissipation. The dissipation is notably high, given that the structural members remain essentially elastic, and therefore provides essentially no hysteretic energy dissipation. Furthermore, the straight tendon profile in the East-West (seismic) direction results in very low friction between the duct and tendons and therefore also contribute very little inherent energy dissipation. The hysteretic results without damper contributions are presented in Rodgers (2009), and show an essentially bi-linear elastic response regime with negligible energy dissipation. The specimen did not suffer any noticeable stiffness or strength degradation, and stable hysteretic energy dissipation is evident.”*

On page 15, minimal damage is reported. While that is common in hybrid systems in general, a picture is worth a thousand words - especially for potentially extravagant claims.

- The authors agree that a picture provides significant additional insight to readers. However, the decision was made not to include a picture due to the tight space constraints. The following figure shows the subassembly after testing to 3% drift, with cracks marked. It is evident that only minor flexural cracks exist due to the armouring at the joint interface and damage avoidance design approach.

**The authors have not included this figure in the revised manuscript as it is already at the maximum length. However, they are definitely prepared to add this material at the reviewer's request, subject to the editor's discretion.**



**Figure XX:** Photographs of the specimen after uni-directional Quasi-Static testing: (a) the specimen at approximately 3 percent drift; (b) the west beam after completion of testing.

9. "Multi-level Seismic Performance Assessment". The performance during the "rare" earthquake (2% in 50 years or 2450 year return period) seems suspiciously low, with a drift of only 1.6%, so it is hardly surprising that the damage level was low. Most cast-in-place conventional system also show very little damage at that drift.

- The authors would like to note that in Figure 9, the maximum North-South drift is indeed only approximately 1.7%. However, as this is a bi-directional testing regime, it should be noted that the maximum East-West drift is actually approximately 2.7% in the same figure. Moreover, the total radial drift for the specimen due to the combination of the simultaneous North-South and East-West loading pattern is actually approximately 3.1%. Therefore, while the reviewer has made a correct observation, the other components must be considered and give a more realistic maximum drift.

The authors note that if this aspect was not apparent to the reviewer, then additional discussion on this point must be added to the manuscript for clarity. Therefore, the following addition had been made to the manuscript.



On page 18, where the 90% MCE results are discussed, the sentence which originally read:

*“The displacement demand consisted of one primary pulse to 2.8% interstory drift, followed by several small cycles.”*

Has been modified to:

*“The displacement demand consisted of one primary pulse to 2.8% East-West interstory drift (3.1% radial drift), followed by several small cycles.”*

Stylistic and editorial comments.

\* The extensive use of acronyms is irritating and unnecessary. This is an engineering journal, not a military handbook.

\* In text descriptions, the callout to the figure should be at the start of the description, not at the end. Usually the text description makes more sense if the reader already has in mind a picture of the system or component under discussion.

\* In many instances, words are used incorrectly, omitted or mis-spelled (e.g. "yeilding" on page 3; "tolerances could be considerably less than for fully precast members" page 4; "high performance concrete must be used..." at the top of page 5 - it always can; "hand tightening the nuts (??) anchoring the damper to the beam"; this criterion relates..." page 17; etc., etc.). Careful review by the authors, and possibly by a good technical editor, would help to make the paper easier to understand.

In summary, the paper contains an idea that is technically interesting, although of questionable market value, but the description of it is so hampered by poor explanation that the paper is not publishable in its present form. The authors are encouraged to re-work it so that a reader can understand the system more easily and fully, and then to re-submit the manuscript.

➔ The authors note that the use of acronyms was unnecessarily extensive. Therefore, the use of acronyms has been reduced and eliminated where practical. A few key acronyms are kept where they are used repeatedly to avoid excessive repetition.

## **Reviewer 2:**

Methods to improving seismic performance of precast concrete structures are critical to the industry. This study followed the spirit of PRESSS project with an expectation of advancing the state-of-the-art. The authors proposed and tested putting dampers inside beam-column joints to improve the energy dissipation of precast structures. However, Dampers, both hysteric dampers (e.g., the one in this manuscript) and viscous/friction dampers (velocity dependent devices) need to be placed such that the dampers undergoes large displacement/ velocity during an earthquake. The efficiency of the proposed damping mechanism needs to be studied.

The review of literature is a bit limited to PRESSS related research. A broader review of using damping devices in concrete frame structures can be helpful to position the research. In addition, literature review pertaining to the multi-level seismic performance assessment (MSPA) needs to be added, especially on various pushover analysis and hybrid simulations.

- The authors acknowledge the comments of the reviewer. As such, the following references are added discussing other options that have been investigated for energy dissipation/damping for concrete structures. On page 3 of the manuscript, the following paragraph has been added:

*“Other research has looked at alternatives for providing energy dissipation to concrete structures. Pekcan et al. (1995) examined the use of elastomeric spring dampers to provide energy dissipation. Christopoulos et al (2008) developed a self-centering, energy dissipating bracing system which could be used in either concrete or steel structures, while Shen et al (1995) examine the use of viscoelastic dampers to provide seismic resistance to concrete frames. The development of passive control systems that use yielding steel braces and shape-memory alloys is detailed in Dolce et al. (2005).”*

With the corresponding references added:

Pekcan G, Mander JB, Chen SS. (1995) “The Seismic Response of a 1:3 Scale Model R.C. Structure with Elastomeric Spring Dampers” *Earthquake Spectra* **11**(2):249-267

Christopoulos C, Tremblay R, Kim H-J, Lacerte M. (2008) “Self-Centering Energy Dissipative Bracing System for the Seismic Resistance of Structures: Development and Validation” *Journal of Structural Engineering – ASCE* **134**(1):96-107- DOI: 10.1061/(ASCE)0733-9445(2008)134:1(96)

Shen KL, Soong TT, Chang KC, Lai ML. (1995) “Seismic behaviour of reinforced concrete frame with added viscoelastic dampers” *Engineering Structures*, **17**(5):372-380.

Dolce M, Cardone, D, Ponzo FC, Valente C. (2005) “Shaking table tests on reinforced concrete frames without and with passive control systems” *Earthquake Engineering and Structural Dynamics*. **34**:1687–1717, DOI: 10.1002/eqe.501

- To better describe the MSPA procedure, the explanation has been extended, and clearer citation to the key references in this area are made.

The paragraph on page 13 which originally read:

*“A reliable computational model of the structure yields displacement profiles at nodes of interest for use in physical testing. This task required the identification of earthquakes likely to represent various levels of demand, considering both rare and relatively frequent earthquakes. A procedure described by Dhakal et al. (2006) was adopted to define three key earthquake records representing multiple levels of seismic demand. This procedure consists of performing an Incremental Dynamic Analysis (IDA) (Vamvatsikos and Cornell, 2002) to identify the structural response from various earthquakes. Earthquakes representing percentile levels at various intensities can then be identified and used for subsequent analysis.”*

Has been modified and extended to:

*“In order to perform a Multi-Level Seismic Performance Assessment (MSPA), the earthquake records to be used must be pre-identified. Dhakal et al. (2006) proposed a methodology based on Incremental Dynamic Analysis (IDA), where an IDA is conducted using multiple earthquake ground motions and the IDA results are probabilistically processed to select records that give medium and high confidence at desired levels of seismic intensity. Performing an IDA involves conducting nonlinear dynamic analyses of a computational structural model subjected to a suite of earthquake ground motion records scaled to different intensity measures (IMs) (Vamvatsikos and Cornell, 2002). For each analysis, an engineering demand parameter (EDP) is monitored, producing an IDA curve (i.e. a plot of IM vs EDP) for each earthquake record.*

*A reliable computational model of the structure yields displacement profiles at nodes of interest for use in physical testing. This task required the identification of earthquakes likely to represent various levels of demand, considering both rare and relatively frequent earthquakes. The procedure described by Dhakal et al. (2006) was adopted to define three key earthquake records representing multiple levels of seismic demand, by performing an IDA (Vamvatsikos and Cornell, 2002) to identify the structural response from various earthquakes. Earthquakes representing percentile levels at various intensities can then be identified and used for subsequent analysis.”*

The determination of predicted seismic demands needs more detailed description. It looks like the authors are using the initial stiffness in the calculation while the connection and the structure will have reduced stiffness in an earthquake.

- The reference to the ‘reduced stiffness in an earthquake’ implies that stiffness/strength degradation occurs across multiple loading cycles. The use of an initial stiffness was justified as the specimen exhibited essentially no stiffness degradation across multiple loading cycles, irrespective of the displacement loading profile.

The sentence on page 18 that originally read:

*“The specimen did not suffer any stiffness or strength degradation.”*

Has been modified to:

*“The specimen did not suffer any stiffness or strength degradation, as shown in the experimental results of Figure 6, and in more detail in Rodgers (2009).”*

The following figure (not presented in the manuscript due to length) shows the uni-directional (East-West) loading to 4% drift for both increasing and decreasing drift amplitudes. At each drift increment, two fully reversed cycles are undertaken. It can be seen in the results that there is essentially no difference in the overall connection hysteresis for the increasing and decreasing drift amplitudes.

**The authors have not included these results in the manuscript, but have instead drawn reference to other published work. The authors are prepared to add this figure at the discretion of the reviewer and the editor.**

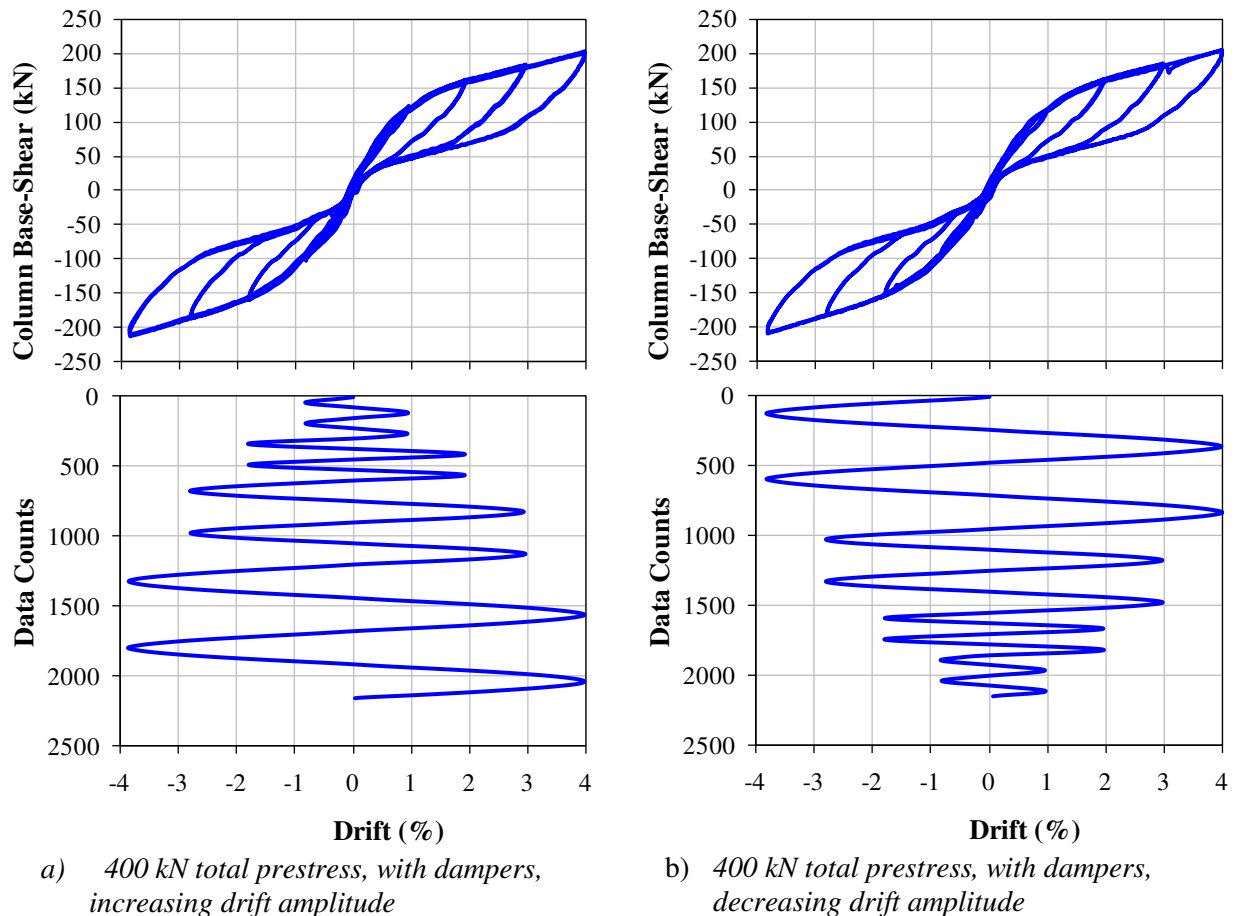


**Figure XX:** Comparison of increasing and decreasing drift amplitudes

This reviewer is very much interested in seeing how the authors select earthquake records (frequency sensitive) and determine the performance demands.

- The records are the SAC suite, and the specific earthquake ground motions are selected based on the 10<sup>th</sup>, 50<sup>th</sup> and 90<sup>th</sup> percentile, as shown in Figure 5. The SAC suite is a standard set chosen by the authors as a standard benchmark. Therefore, they feel that it is outside the scope of this manuscript, particularly in light of the tight page limit, to discuss frequency content of the earthquake.

The standard set of SAC records are used, and the appropriate earthquakes are chosen using the methodology described in the manuscript and shown in Figure 5.

By the way, a 2.8% drift was achieved in the quasi-earthquake displacement tests (Fig. 9) while a 4% drift was claimed in the conclusion.

- The reviewer raises a very good point. The total radial drift in Figure 9 is actually approximately 3.1% when the North-South component is considered in addition to the 2.8% East-West drift. However, the claim of 4% in the conclusions is an error. The results presented below were originally included, but they were omitted as the manuscript was over-length.

Therefore, while a total radial drift of approximately 4.2% has been undertaken and showed little damage, the authors recognise that that claim clearly cannot be made without the supporting evidence. Therefore, in light of the removal of these results from the submitted manuscript, the corresponding claim must also be removed. The authors thank the reviewer for noticing this oversight. Therefore, the section at the end of the conclusions which originally read:

*“Throughout QS and QED testing up to 4% radial drift the specimen suffered negligible damage; only some small cracks were observed near the steel armouring and these generally closed after testing.”*

Has been modified to read:

*“Throughout quasi-static and QED testing up to 3.1% radial drift the specimen suffered negligible damage; only some small cracks were observed near the steel armouring and these generally closed after testing.”*

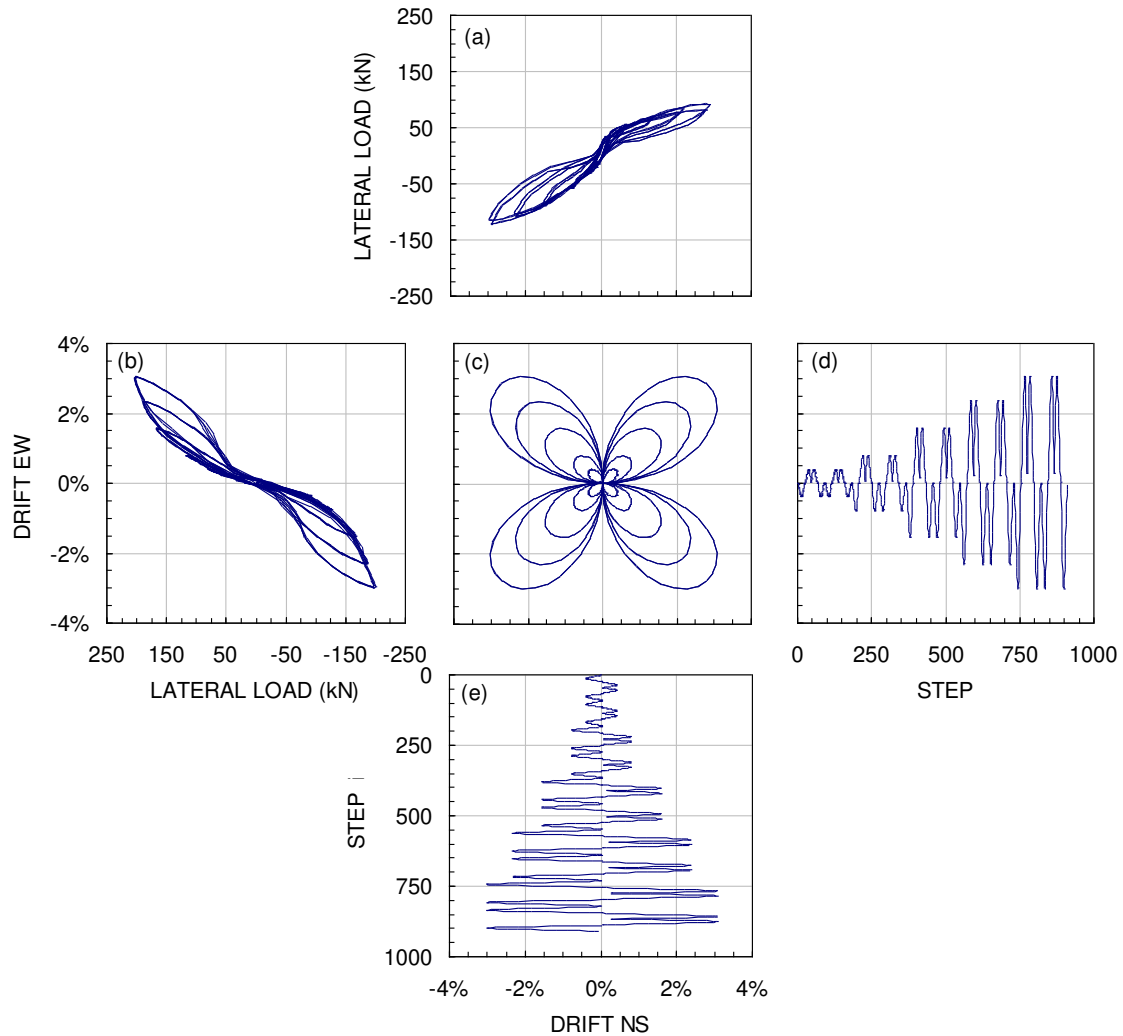


**Figure XX:** Bi-direction QS testing to 4 percent drift: (a) and (b) give the force-displacement response in the NS and EW direction, respectively; (c) shows a plan view of bi-directional orbit; (d) and (e) give the displacement profiles in the EW and NS directions, respectively.

**The authors have not included this figure in the revised manuscript as it is already at the maximum length, and have instead drawn reference to the thesis in which it is presented. However, they are definitely prepared to add this material at the reviewer's request, subject to the editor's discretion.**

It is desirable to show rate-dependent behavior of the HF2V damper in Fig. 4. In addition, the gradual reduction of the residual damping force (12 years needed based upon the proposed model) and its impact to the joint behavior is needed. It is likely to have a medium drift that may cause damper yielding before the major drift during an earthquake.

- ➔ The velocity dependence is presented in another article currently in press in this same journal. While the authors agree with the reviewer, and would like to include this information, the tight page limit for this journal precludes the addition of this figure. Instead reference is drawn to the other paper, and a relevant thesis, which will soon be available on the institutional repository.

At the end of the paragraph immediately following Equation (1) in the manuscript, the following sentence has been added:

*“More detailed velocity dependence studies can be found in Mander et al. (2009), and Rodgers (2009).”*

The authors would also like to reiterate that the dampers do not ‘yield’ as such, and while they undergo displacements that induce plastic deformation within the lead, subsequent cycles are not effected by the smaller, or larger previous cycles. This phenomenon was shown in the response to a prior query from this reviewer, where the overall joint behaviour for both increasing and decreasing drift cycles was shown.

The comment on the constructivity is very helpful. It is also desired to comment on the size effect of the proposed mechanism: is a full-size joint with larger size damper going to behave similarly?

- ➔ The overall joint behaviour is a combination of elastic member stiffness, level of post-tensioning and damper forces. The specific hysteretic behaviour is therefore a result of the relative contributions. The prediction of larger connection designs can be accurately predicted based on the Menegotto-Pinto models of Li (2006), Solberg (2007) and Rodgers (2009).

The references are:

*Li, L., (2006), “Further experiments on the seismic performance of structural concrete beam-column joints designed in accordance with the principles of damage avoidance”, Master of Engineering Thesis. Dept. of Civil Engineering, University of Canterbury, Christchurch, New Zealand. <http://ir.canterbury.ac.nz/handle/10092/1098>*

*Solberg KM. 2007. Experimental and Financial Investigations into the further development of Damage Avoidance Design. Master of Engineering Thesis. Dept. of Civil Engineering, University of Canterbury, Christchurch, New Zealand. <http://ir.canterbury.ac.nz/handle/10092/1162>*

*Rodgers, G. W. (2009) “Next Generation Structural Technologies: Implementing High Force-to-Volume Energy Absorbers” PhD Thesis, Dept. of Mechanical Engineering, University of Canterbury, Christchurch, New Zealand.*